FH Aachen University of Applied Sciences
Department of Aerospace Engineering

Bachelor Thesis

Design, Specification, and Implementation of the Martian Moons Exploration Rover's Separation Test

Ole Springer

Matriculation Number: 3115664

First Examiner: Prof. Dr.-Ing Bernd Dachwald

Second Examiner: Jan-Thimo Grundmann

Bibliographic Information

Author:	Ole Springer 19.09.1996 in Hamburg
Title:	Design, Specification, and Implementation of the Martian Moons Exploration Rover's Separation Test
Document type:	Bachelor Thesis
Study course:	Luft- und Raumfahrttechnik
Cooperation:	**UAS Aachen (FH Aachen)** Department of Aerospace Engineering Institute for Space Systems **German Aerospace Center (DLR)** Institute for Space Systems Bremen
Date of completion:	July 1st, 2022
Keywords:	MMX, ROVER, PHOBOS, MARS JAXA, DLR, CNES, HDRM, SEPARATION, TEST

Declaration of Independence

I hereby declare that I have written this thesis independently within the framework of the usual care and have not used any sources or aids other than those indicated.

All text passages taken verbatim and in spirit from external sources have been marked.

The work has not been submitted in the same or similar form to any other examination authority.

Bremen, 01.07.2022

Ole Springer

Acknowledgement

I would like to take this opportunity to thank Mr. Jan Thimo Grundmann. Not only for the opportunity and the trust he has shown me from the beginning, but also for the extensive support throughout my thesis. The meetings regarding the concept and the implementation of the topic were very informative and of great benefit to me.

Furthermore, I would like to thank all my colleagues at DLR, who have been unbelievably open and helpful. The exchange with you was very inspiring and I learned so much. Special thanks to Mr. Siebo Reershemius, whose experience in the field of separation mechanisms was very helpful for this thesis.

Abstract

As part of the Martian Moons Exploration mission, the MMX rover will land on the Martian moon Phobos. The rover has to be separated from the spacecraft to touch down on the surface shortly afterwards. To validate the reliability of this separation as well as to ensure that the requirements are fulfilled, the separation must be tested many times. To perform these tests cost- and time-effectively, the single-use separation mechanisms were exchanged for reusable ones for the tests. To actuate these mechanisms, an additional support structure had to be designed to meet the demands. This thesis presents the concept for this support structure and explains the exact adjustments that have to be made on the test subject as well as on the existing test equipment. The required components for the structure were selected and all necessary dimensioning was carried out. Additionally, the exact test environment and the measuring instruments that will be used are described. All scenarios to be tested were introduced and the possibility to test them was considered in the concept. Unfortunately, a complete implementation of the concept and the execution of the separation tests itself could not be realized and documented in this thesis due to massive delays in the test schedule. Nevertheless, all possible arrangements have been made to start the implementation of the support structure and begin the separation tests as soon as external circumstances will allow.

Scope of Work

This thesis deals with the separation tests of the MMX rover. For those tests a reusable version of the separation mechanisms is used to keep the costs low. The reason for this is the high number of separations required and the resulting lower costs compared to disposable mechanisms. Therefore, a more complex test support structure is required, due to the altered type of triggering. The design will be explained in more detail starting in Chapter 3. The elaboration of the different scenarios to be tested is also part of the work. In addition to the normal separations, special cases are also simulated, which investigate possible impacts of partial malfunction during the separation. Besides that, the documentation of the test procedure, the used instruments and description of the test environment is also part of this thesis. The given requirements must be met and the possibility to reuse the setup for later COR tests should be taken into account in the design.

Contents

1 Introduction

1.1 Mission

The Martian Moons Exploration (MMX) Mission by the Japanese Aerospace Exploration Agency (JAXA) will be launched to the Martian moons Phobos and Deimos in September 2024. The goal is to better understand the moons, as there are different theories about their origin. Launched by an H3-24L rocket which is currently under development, the spacecraft with a total wet mass of about 4000 kg will be sent onto a Hohmann-like transfer-orbit to Mars [1].
After a cruise of about eleven months the spacecraft will arrive at Mars in August 2025. During its three year stay the MMX spacecraft will primarily observe Phobos and Deimos, but also the circum-Martian space as well as the atmosphere of Mars. Another part of the MMX mission is the deployment of the MMX Rover, which will be introduced in Chapter 1.2. The close observation of Phobos will also help to determine possible landing sites. Subsequently, the spacecraft will land on two different sites to take some samples from the surface. Afterwards, it will do multiple flybys of Deimos before leaving the Martian system, heading back to Earth, where return of the spacecraft and its surface samples is expected in the year 2029 [1].

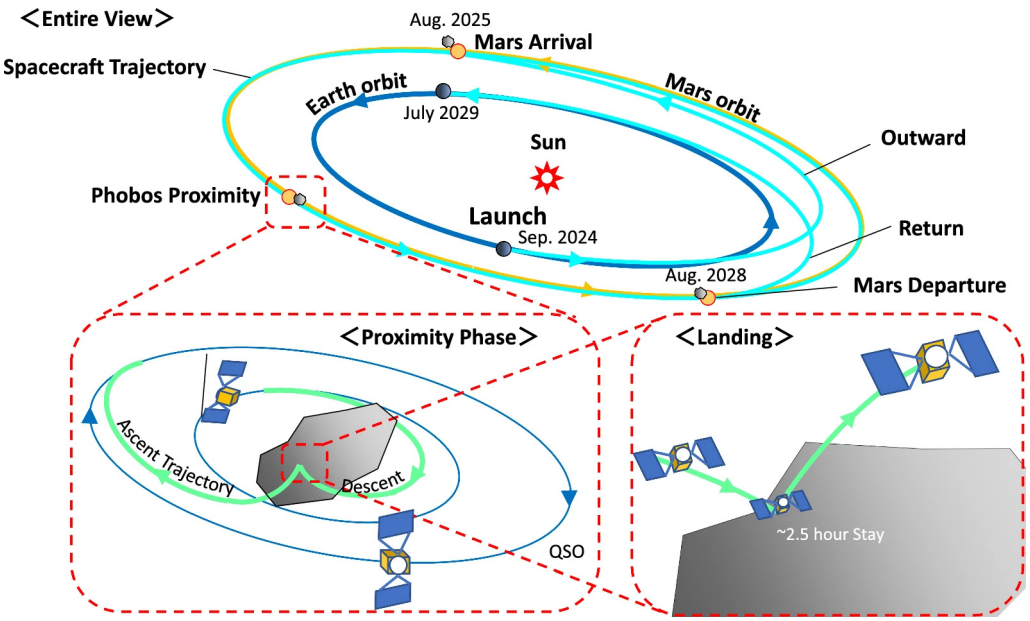

Figure 1: Mission profile of the MMX spacecraft [1].

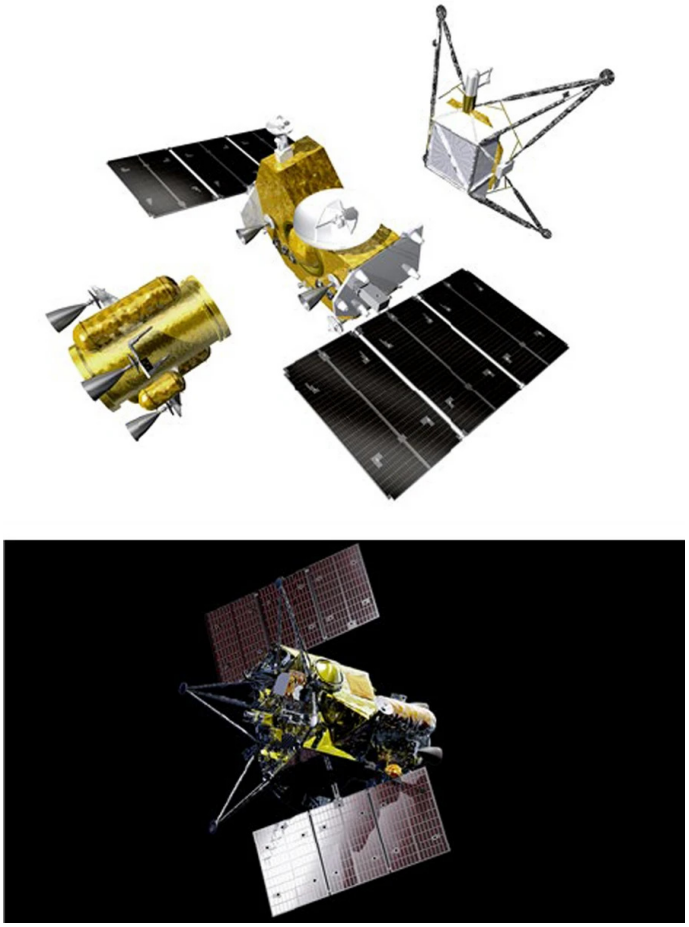

Figure 2: The current design of MMX spacecraft.
From left to right, propulsion, exploration, and return modules (top).
On-orbit configuration (bottom). The size of a solar panel is 2.4 m×4.4 m [1].

1.2 Rover

The french National Centre for Space Studies (CNES) and German Aerospace Center (DLR) joined forces to contribute a rover to the MMX mission. Its total mass is about 25 kg [2]. The box-shaped design is 310 mm in height, 375 mm in width, and 445 mm in length [3]. While CNES is responsible for providing the scientific cameras and the Service Module (SEM), DLR's part is to design, manufacture, integrate, and test the rover's structure and provide two instruments; the Raman spectrometer instrument (RAX) and the thermal infrared radiometer (miniRad). The composite parts of the structure are manufactured at DLR's Institute of Composite Structures and Adaptive Systems in Braunschweig, Germany. Assembly, integration and testing takes place at DLR's Institute of Space Systems in Bremen, Germany. DLR's Institute of Robotics and Mechatronics in Wessling, Germany will provide the locomotion including all four wheels, each located at the end of a leg. The legs are

pivoted at the rover and allow the rover to be lowered and tilted. Thus, the rover can align the solar panels toward the sun as well as lower itself for surface experiments of the RAX.

RAX is one of four instruments on board of the rover. To do scientific research, the legs will rotate, so the instrument's distance to the surface will be decreased until it is within its working distance. Then RAX will perform Raman spectroscopic measurements to identify the mineralogy of Phobos' surface [2].

Another instrument is the NavCAM. Two cameras point in the direction of travel and are arranged to provide a three-dimensional view. This view is important because these cameras are used for autonomous navigation as well as taking images of the landscape, which will help to better understand the surface materials composition. The stereo camera setup will also provide vital data to determine the orientation of the rover [3].

Besides the two cameras of NavCAM there will be another two called WheelCams. One camera observing the left front wheel and one the left rear wheel. As the rover moves, the interaction between wheel and surface material of Phobos can be studied closely. This data will also provide additional knowledge about properties of the regolith, which may reduce the MMX spacecraft's risk during landing and sample collection [2].

The miniRad instrument is able to measure the surface brightness temperature and determine thermal properties of the surface of Phobos. "The radiometer field of view will be located within the field of view of the stereo navigation cameras (NavCams), which will provide context for the brightness temperature measurements" [4].

Shutters are provided to protect the instruments from dust. They are preloaded by a spring and swing open as soon as the retaining bolts are triggered. This action takes place after the rover has landed, the wheels were extended and dust kicked up by the landing has settled.

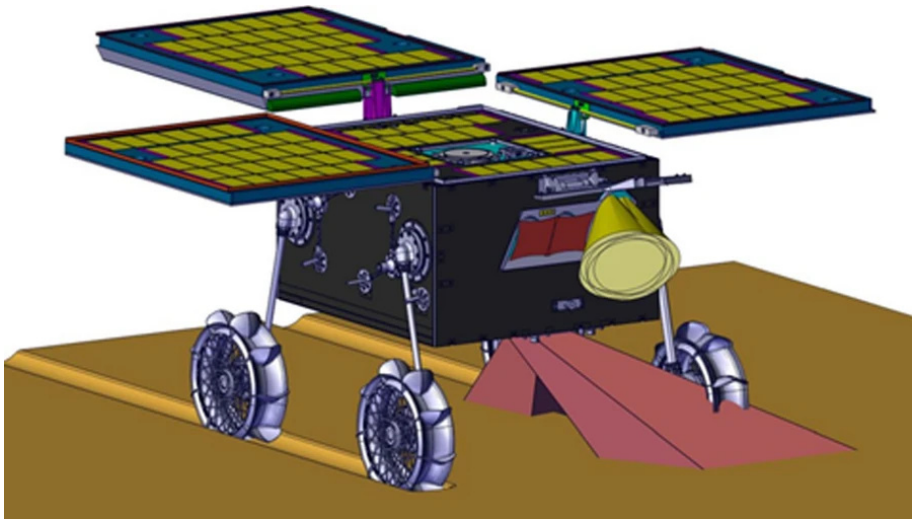

Figure 3: MMX rover with deployed wheels and solar panels in the on-surface configuration. Field of views of miniRad and Wheelcams are indicated in yellow and red, respectively [5].

As shown in Figure 3, the rover has three solar panels in order to recharge the battery and provide enough power for the scientific actions during the planned mission duration of at least 100 days. They are securely folded on top of the rover during its cruise and landing phase. Shortly after landing, the panels will be deployed.

1.2.1 Mechanical and Electrical Chassis Support System

The Mechanical and Electrical Chassis Support System (MECSS) is the interface between rover and MMX spacecraft. It is - like the rover itself - box-shaped and has similar dimensions with a total mass of about 2.3 kg [2]. As long as the rover is attached to the main spacecraft, data and power exchange is ensured through the umbilical connector which is located in the middle of the MECSS and rover, respectively. Four bolts, one at each corner, hold the MECSS securely to the MMX spacecraft. Next to each bolt, the Hold Down and Release Mechanism (HDRM) is embedded in the MECSS structure. Those keep the MECSS and rover mechanically connected and can be triggered to detach the rover at given time. They will be described in more detail in Chapter 1.3.1. Additionally, an x-shaped Push-Off Plate (POP) is located at the center of the MECSS. It is secured with a bayonet-like lock, containing a spring, completing the Push-Off Mechanism (POM). This lock is shown in Figure 4 next to the pink protective cap of the umbilical connector. During mating the plate is pushed down by the bottom-plate of the rover, compressing the spring.

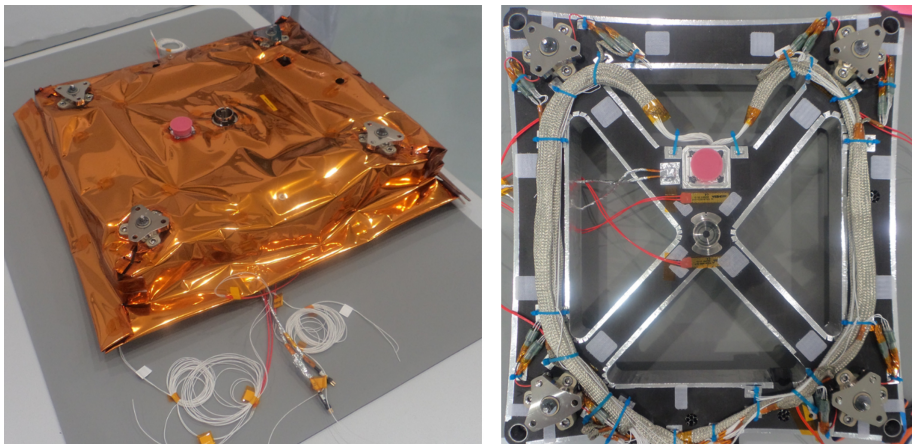

Figure 4: MECSS Qualification Model (QM)1 ready for testing with MECSS Multi Layer Insulation (MLI) fitted (left) and without (right).

1.3 Separation and landing

During cruise phase, the rover is attached to the bottom of the spacecraft's return section, which is shown in Figure 2 and 5. As part of the MMX mission, the rover will be dropped onto the surface of Phobos.

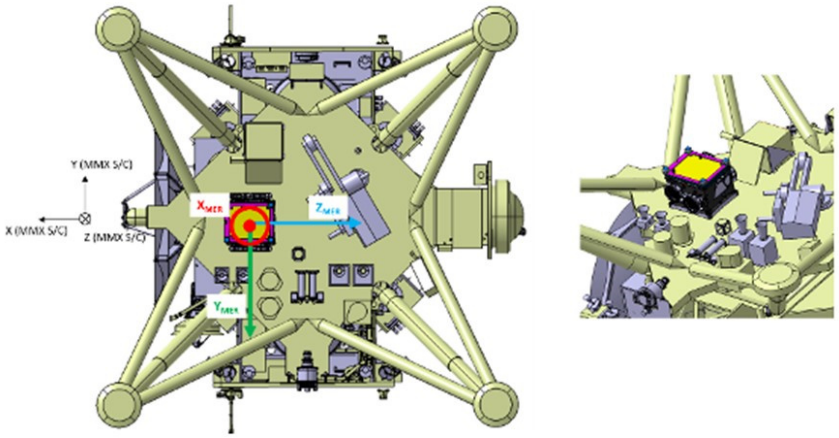

Figure 5: The Rovers position at the bottom of the MMX spacecraft.

As previously mentioned in Chapter 1.2, one of the rover's main objectives is to minimize the risk for the landing and sample collection of the MMX spacecraft. Thus, the rover will be deployed first [6]. Therefore, the MMX spacecraft decreases its altitude below 100 m (45 m is expected as of the publication of this thesis) and fires the HDRMs on each corner of the MECSS. Most of the push-off force is applied by the push-off plate. It is used to separate the rover from the spacecraft in a controlled

manner. Besides the force provided by the spring inside this push-off mechanism, there are two other factors that contribute to the push-off.
Firstly, the remaining parts of the bolts, which are held by the HDRMs and are pulled into the rover as soon as the mechanism is released, as shown in Figure 7. This initially generates a force against separation. However, when the pin reaches the stop, the momentum generated by the bolt and spring mass helps with the separation.
And secondly, the compressive forces of the contact pins of the umbilical connector. All three factors are playing part in pushing the rover away from the MMX spacecraft. Thus, they must be taken into account when investigating the separation behavior.

After separation, the rover is in a ballistic free fall until it makes first contact with the surface of Phobos. Due to Phobos' small average radius of 11.08 km and thus its low gravity, the weight of the rover will be about 2000 times smaller than it would be on Earth [6]. Since there is no attitude control system during the descent, the rover could reach the surface in any position. After hitting the surface at approximately 1 meter per second, the rover is expected to bounce several times before finally coming to rest [5] [7]. The deployment of the wheels will upright the rover regardless of its attitude. Once the rover is upright standing with its wheels on Phobos the solar arrays and shutters can be unfolded [6].

1.3.1 Hold-Down and Release Mechanism

The Hold-Down and Release Mechanisms are - besides the umbilical connector and POM - the only mechanical connection between MECSS and rover. Unlike the other connections, which are frictional connections, the purpose of the HDRMs is to hold the rover secured during cruise phase and release it reliably at a given time. The HDRM consists of the cup-cone interface and the release unit, the Hold Down and Release Component (HDRC). HDRCs, including the 061-005 by Glenair used on this mission, are off-the-shelf components. A similar working component has already been used on the MASCOT lander although the arrangement and design of the HDRMs cup-cone interfaces differed. For example, MASCOT used only a single, central HDRM while the MMX rover is kept in place by four, located at the corners.

Figure 6 shows the assembly of an HDRM at different stages. A bolt is held by the mechanisms and leads out of the center of the case. It has an internal thread, into which a threaded rod can be screwed. The so-called cup-cone interface is necessary to distribute the hold-down forces and prevent sticking between rover and MECSS

during separation. Additionally, cup and cone are coated differently to minimize friction and prevent cold welding. The MECSS-sided cup and the (shiny) rover-sided cone are also shown in Figure 6. Screws through the three holes of the cone attach the interface to the rover. A similar setup is used to secure the cup on the MECSS. A special apparatus is used to preload the spring inside the mechanisms to 13 kN. This will help to pull the released bolt out of the triggered HDRM.

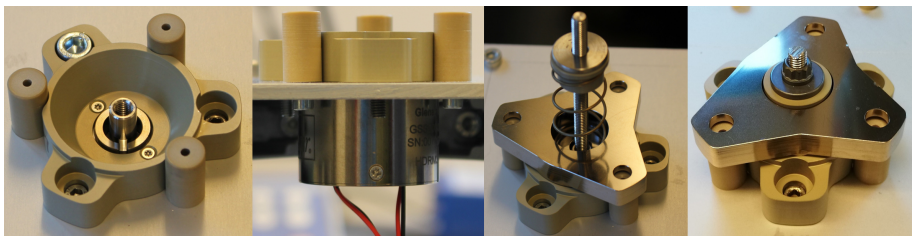

Figure 6: HDRM at different stages during assembly. Far right, a fully assembled one.

To release the bolt it is necessary to cut a thin wire wrapped around two semicircular shells. Therefore, a short electric pulse is applied to the wire, causing it to melt. If the first pulse is unsuccessful a second pulse is fired shortly thereafter through a second, separate circuit. Once the wire is cut, the shells are no longer held together and the bolt comes loose. This can be seen in Figure 7.

2 Problem

The Hold-Down and Release Mechanism, as described in the previous Chapter 1.3.1 is extremely reliable because there are no moving parts to wear out or seize up during a long cruise phase. A thin wire is melted to trigger the HDRM. Once the wire has melted, the mechanism has done its job and is no longer usable.

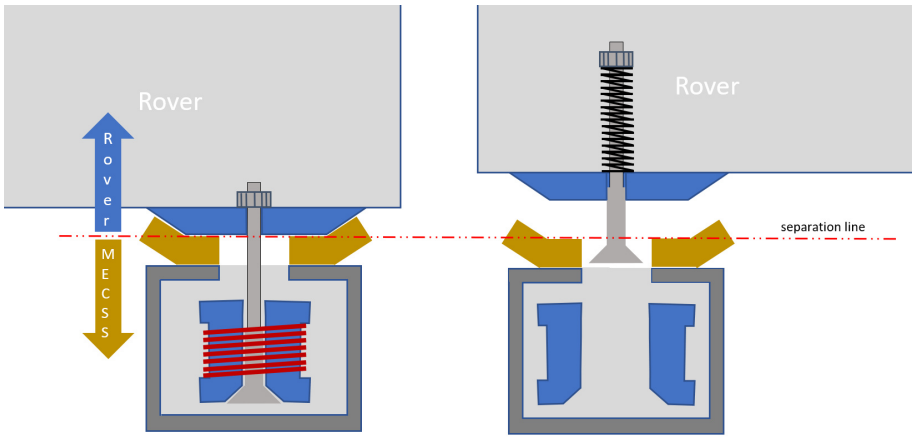

Figure 7: Simplified representation of a Glenair HDRM 061-005 in hold-down (left) and release (right) phase.

Instead of being fired only once to separate as envisioned in the mission profile, separation must be performed multiple times during the test campaign to validate the reliability of the separation process. The exact number is not set at the time of this publication, but is in the range of 15 to 35. This includes various scenarios in which the system behaves abnormally, to determine the impact of these errors in terms of separation. More about this in Chapter 6.5. With four HDRMs needed for each separation, it results in a total of more than 100. Using these would be very expensive, thus an alternative is needed. Fortunately, Glenair already provides a solution to this problem by offering a version of their HDRM, that is designed for reusable use. This version does not require cutting a thin wire to release the retaining bolt. Instead, the mechanism is triggered by a normal wrench. Chapter 3.1 takes a closer look at how it works and the problems it causes.

Since the HDRM is now triggered externally, an additional support structure is needed. It must serve both, as a fixed mounting for the MECSS, and support the external release mechanism. The concept and the design of this support structure is an essential part of this thesis and is explained in more detail in the following Chapter 3.

3 Concept

The separation tests are the final of the whole test campaign, including vibration, shock and thermal vacuum tests. They are performed with the second Structure Model (SM) of the rover. Even if the SM2 follows the approach of being as flight-like as possible, most parts and instruments are only represented by a mass dummy with similar dimensions. The SM2 can be broken down into two assemblies. One assembly is the MECSS, which was introduced in Chapter 1.2.1. The other one is the rover model. Thus, the rover itself is also referred to as the Pre-Assembled Chassis (PAC) in the context of the separation tests. This is to clarify which components are meant specifically as well as indicate that most of the instruments are still missing or represented by mass and dimension dummies.

3.1 Substitute for the Hold Down and Release Mechanism

Since the reusable HDRM version is used in the separation tests, an external support structure is needed for the HDRM to be triggered, because of its alternative trigger mechanism. Instead of melting a wire inside, the reusable version of the HDRM is triggered differently. As shown in following Figure 8, the flight version has two pairs of cables coming out of the back. One for the main circuit, the other one for the redundant backup.

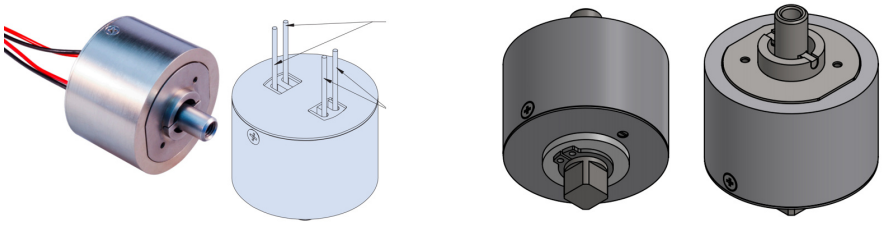

Figure 8: Flight version Glenair HDRM 061-005 (left) with electrical trigger wires (arrows). Reusable version as used in separation tests (right)[8].

The reusable version has a rectangular wrench size 8 interface. By turning this by about 90 degrees, the retaining bolt is released and retracted due to the preloaded spring. This version of the HDRM is - like the flight version 061-005 - developed by Glenair and can be bought off-the-shelf. Except for its trigger, there is no difference to the flight version, meaning that as written in Chapter 1.3.1 the same apparatus is used to tension the spring inside the mechanism to 13 kN. Same applies to the cup-cone interface. Anything that deviates from the actual flight profile may cause

errors or even hide them. Thus, it is important to have as few differences as possible to the flight version, so the test results represents reality. However, this "reusable" triggering also causes some problems.

For the flight version it is easy to determine when the wire inside the mechanism is cut. The required electric pulse takes only fractions of a second to melt the wire and release the bolt [8]. Determining this for the reusable version proves to be more difficult. The mechanism will release the bolt somewhere along the 90° turn. It is a range of angles, rather than an exact angle. Thus, it is also impossible to determine an exact point in time. It is rather a time period in which the release will take place. Therefore, it is very difficult to identify the specific time and position of the rectangular interface when the bolt is released. Position and time, as well as the required torque, also differ between triggers. This was already evident in the initial tests and is described in more detail in Chapter 4.1.

3.2 Mechanical Ground Support Equipment

The previous Chapter 3.1 describes how the reusable version of the HDRC works, what the differences are, and what problems have to be overcome. In this Chapter the Mechanical Ground Support Equipment (MGSE) of the test campaign is introduced.

The MGSE should be capable of the following:

- Suspension for the MECSS in 0° and 90° position
- Ability to trigger all four HDRMs simultaneously
- Possibility to trigger some HDRMs with a delay
- Provide mounting options for measuring instruments and cameras
- Use of as many standard components as possible to keep the costs low and be able to adapt quickly.
- Possibility for continued usage of the MGSE for the Coefficient of Restitution (COR) tests that may take place later on.

The MGSE can be broken down into two major parts. One part of it is the external trigger support structure. It includes everything necessary to actuate the HDRM.

The other part is the modified Weight Compensation Instrument (WCI). The main task of this is to provide the support structure to which the trigger and drop weight - introduced in the upcoming paragraph - can be attached. Furthermore, the WCI can also serves as mounting points for measuring instruments and cameras.

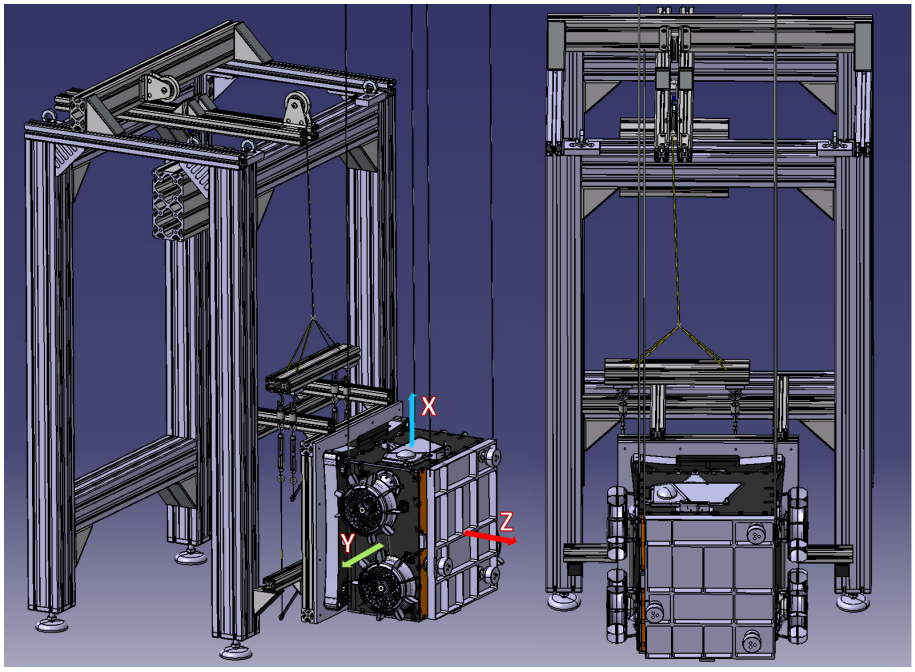

Figure 9: Complete test MGSE with attached MECSS and PAC. Additionally the coordinate system used can be seen.

The basic principle of the test setup is as follows. A weight is released from a certain height. After the weight has been accelerated by the free fall for about 0.4 s, this weight pulls on a steel cable (Refer to Chapter 4.2). The cable runs over two pulleys and is connected to a beam that transmits the force to four other steel cables. These cables lead to wrenches and cause them to rotate, thus triggering the HDRM. The impulse generated by the free-fall ensures that the release is as fast as possible and therefore the delay between individual HDRMs is kept to a minimum. Since the mass of the rover is much lower compared to the MMX spacecraft, the recoil effect during separation can be neglected. Therefore, the MECSS can remain stationary at the MGSE while the PAC is moving after separation. In addition to the 0° position as shown in Figure 9, the structure should also allow to test the separation in a position rotated around the Z axis by 90°. The detailed test scenarios can be found in Chapter 6.5. In the following Chapter 3.2.1 and 3.2.2 the design and the way it works is described in more detail.

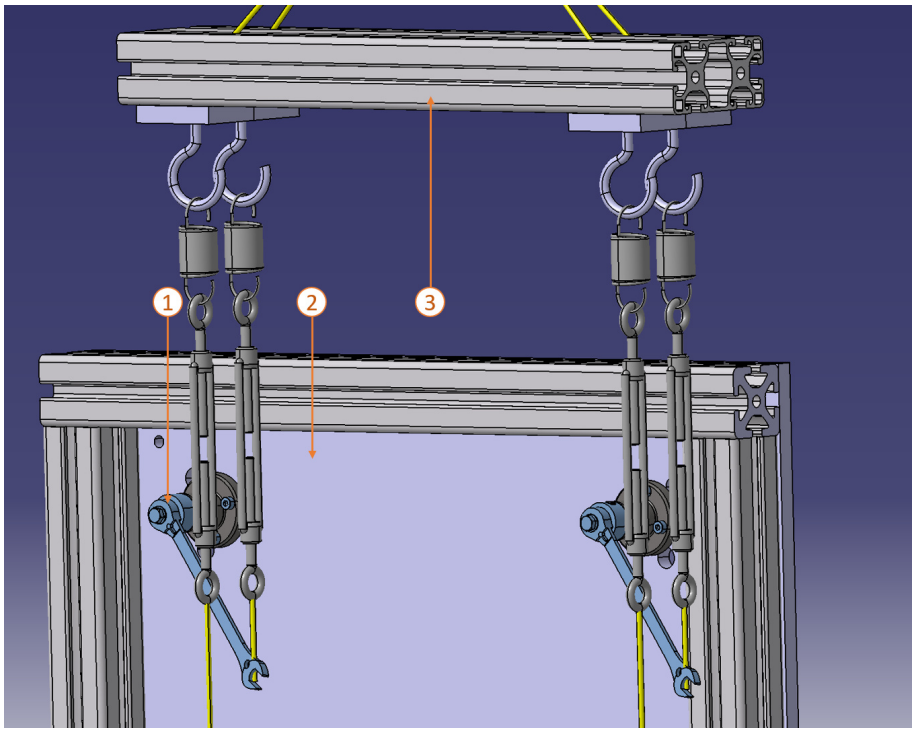

Figure 10: Overview of the external trigger with the lever interface assemblies (1), integrated into the spacecraft simulator plate (2) and the connecting beam (3).

3.2.1 External Trigger

The external trigger support structure introduced in this chapter is essential to perform the separation tests with the reusable version of the Glenair HDRM. The advantage of being reusable is accompanied by some disadvantages, as already described in Chapter 3.1. Thus, the mechanism can only be triggered mechanically, unlike the flight version, which is triggered electrically. And as explained in more detail in Chapter 4.1, the triggering must happen very quickly to keep the triggering delay among the mechanisms to a minimum. Taking this into account makes it a difficult task, while the main requirement for the test scenarios must of course still be met. In the following, the whole assembly of the external trigger and its sub-assemblies are described. In order to keep costs low and delivery time short, standard parts are used at every opportunity. The exact designations and specifications for each of those parts can be found in the appendix. A general summary of all parts of each sub-assembly can also be obtained from the upcoming Tables 3.2, 3.3, 3.4, as well as Table 3.5 in Chapter 3.2.2 for the modification of the WCI.

The external trigger support structure can be broken down as shown in Table 3.1 below.

Pos.	Name	Quantity
1	Lever Interface Assembly	2x long version 2x short version
2	Spacecraft Simulator Plate	1
3	Connecting Beam	1

Table 3.1: main sub-assemblies of the external trigger support structure.

Lever Interface Assembly

For this assembly following parts as shown in Table 3.2 are required.

Pos.	Name	Distributor	Dimension	Qty.	Must be modified
1	square socket wrench	Amf	Size 8 $OD = 16\,\text{mm}$	4	✓
2	SWM-12 shaft	Igus	$D = 12\,\text{mm}$ $L = 1000\,\text{mm}$	1	✓
3	FJUM-01-12-LL	Igus	$ID = 12\,\text{mm}$	4	✗
4	ISO 7092 washer		5x9	8	✓
5	DIN 705-A adjusting ring		12x12x22	4	✗
6	ISO 4762 screw		M4x20	16	✗
7	ISO 4762 screw		M2.5x6	4	✗
8	ISO 4017 bolt grade A		M5x25	4	✗
9	ISO 4032 nut grade A		M5	4	✗
10	ISO 7090 washer grade A		5x10	4	✗
11	467 ratchet combination wrench	Facom	Size 8 $L = 140\,\text{mm}$	4	✗

Table 3.2: Parts list of the lever interface assembly.

In order to trigger the HDRM, the rectangular interface of it must be rotated by a maximum of 90 degrees. This interface of rectangular shape has a wrench size of 8, thus an edge length of 8 mm, hence a diagonal of slightly more than 11 mm. To fit into the plain bearing, an outer diameter of exact 12 mm is required. However, with a required inner diameter of more than 11 mm, the wall thickness would be too small, so the attachment would have to be thicker and thus no longer fit into the bearing. As a result, the square socket wrench, mentioned before in Table 3.2, is

used as the direct attachment (1) to the HDRC. It has an outer diameter of 16 mm and is fixed on a 12 mm shaft that leads through the plain bearing.

There will be two versions of the assembly. A CAD view of the short version lever interface assembly is shown in Figure 11. The length of the shaft is the only difference. For the short version, a 56 mm long shaft is used, a 96 mm long shaft is used for the long version. In order for the shafts to fit into the attachment, the diameter of the first 10 mm must be reduced from 12 mm to 8 mm. Since the machining can be made more efficient with the lathe, the shaft will remain round at the end and will not be milled to the rectangular profile of the attachment. This is because there is a risk that the rotation axis of the shaft will no longer be centered after milling, due to the lack of precision of the existing machine. However, this means that the shape of the shaft itself cannot transmit the torque, thus a screw (2) is needed to secure it. For this, the attachment must first be shortened to 25 mm. Additionally, a through-hole must be drilled from the side, where the screw that is supposed to secure the joint can be inserted later. To ensure sufficient margin against shearing, screws must be attached from both sides or a single through-bolt must be counter-screwed from the other side with a nut. The socket wrench attachment (1) is wider than the bearing. Thus, axial displacement away from the HDRM is impossible. On the other side of the bearing, an adjustment ring (3) is placed onto the shaft. In this way, the displacement in the other direction is also blocked. This displacement is normally blocked by the HDRM from the other side. Thus, the ring is only relevant when MECSS with its HDRMs is not attached. A joint is needed at the end of the shaft in order to turn the shaft by using a ratchet wrench. As mentioned in the previous paragraph, milling is not an option to shape the end of the shaft as desired. There is a lack of personnel and machinery to accomplish this with the required precision. To keep costs low, standard parts are used wherever possible. First, a standard M5 thread is drilled 20 mm deep into the side facing away from the HDRM. The washer (6) from position 10 in Table 3.2 is now placed on the M5x25 bolt from position 8. In the next step, the M5 nut (5) is screwed onto the bolt. For this, it is important to use the ISO 4017 bolt with a thread up to the head instead of the more common ISO 4014 bolt. To leave enough space for the wrench, two more ISO 7092 washers (4) are now placed on the bolts. These are already small but still need to be sanded down a bit to get the outer diameter to 8 mm so that the wrenches are not blocked by them. In the end, the ratchet wrench is placed onto the nut before the whole bolt is screwed into the drilled hole of the shaft. Thereby, the wrench is kept between shaft and washer and cannot slip off. The ratchet of the wrench allows to adjust the wrench's angle in steps of five degrees, with respect to the rest of the trigger setup. Different views of the assembly can be seen in Figure 11.

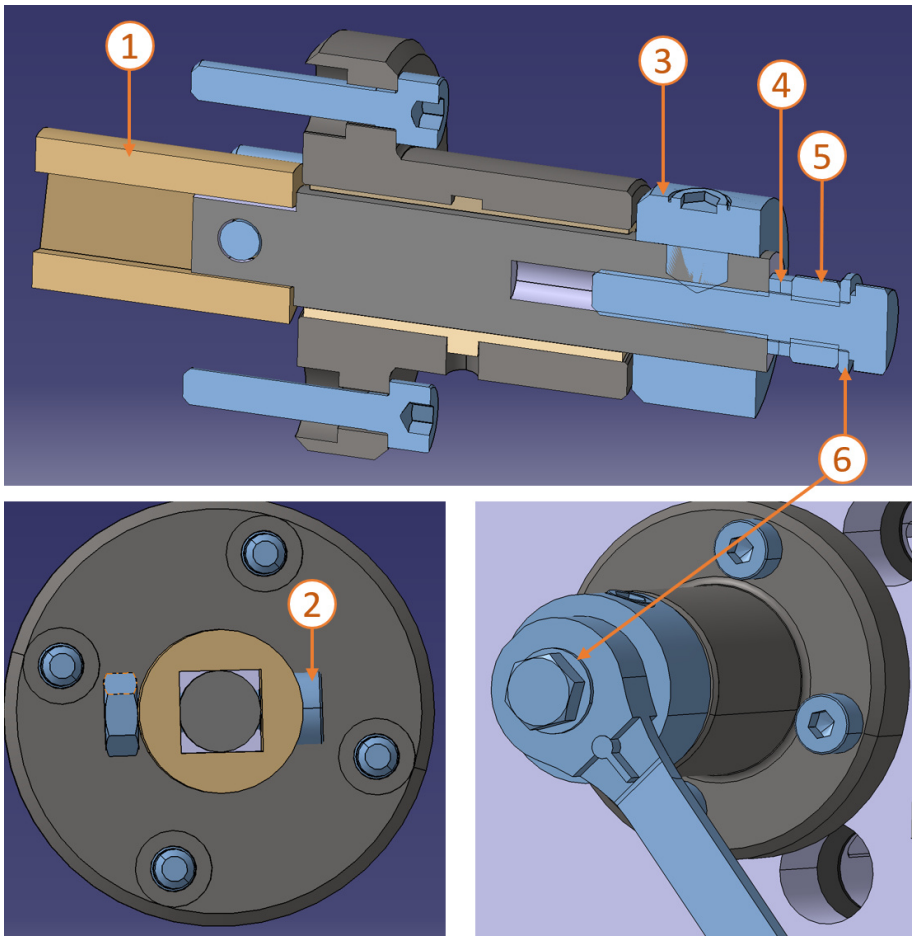

Figure 11: Normal and sectional view of the short version of the lever interface assembly. Square socket attachment (1), locking screw (2), adjusting ring (3), ISO 7092 washer(4), M5 nut (5), ISO 7090 washer (6).

The direction in which the wrench is released is also the direction in which the screw is loosened. This means that it must also be secured by a locking screw. As mentioned before, there are four lever interface assemblies in two different versions. Two are assembled as shown in Figure 11 and another two with a shaft length of 96 mm instead of 56 mm. In the shortened version, the screw head of the locking screw as it was used for the attachment on the other side of the shaft would collide with the adjusting ring, thus a grub screw is used instead. Again, a hole is drilled in the side of the shaft about 15 mm from the edge. After the bolt is screwed into the shaft, a smaller drill is used to make a small cavity in the screwed-in bolt through the grub screw hole. This should give the grub screw more grip later on. It is important that this step does not damage the thread for the grub screw. The grub screw can then be inserted and the adjusting ring fitted onto the shaft. In the long shaft lever version, the assembly order of the grub screw and the adjusting ring is irrelevant as there is no conflict here.

Now that the lever has been assembled it is screwed onto the spacecraft simulator plate. For this however the plate must first be assembled.

Spacecraft Simulator Plate

For the assembly of the spacecraft simulator plate the parts shown in Table 3.3, are required.

Pos.	**Name**	**Distributor**	**Dimension**	**Qty.**
1	Milled plate	247tailorsteel	$h = 530\,\text{mm}$ $w = 500\,\text{mm}$ $t = 10\,\text{mm}$	1
2	Profile 8 40x40	Item	$L = 420\,\text{mm}$	2
3	Profile 8 40x40	Item	$L = 500\,\text{mm}$	2
4	Automatic-fastening set 8	Item		8
5	ISO 4762 screw		M6x20	12
6	ISO 7091 washer		M6	12

Table 3.3: Parts list of the spacecraft simulator plate assembly.

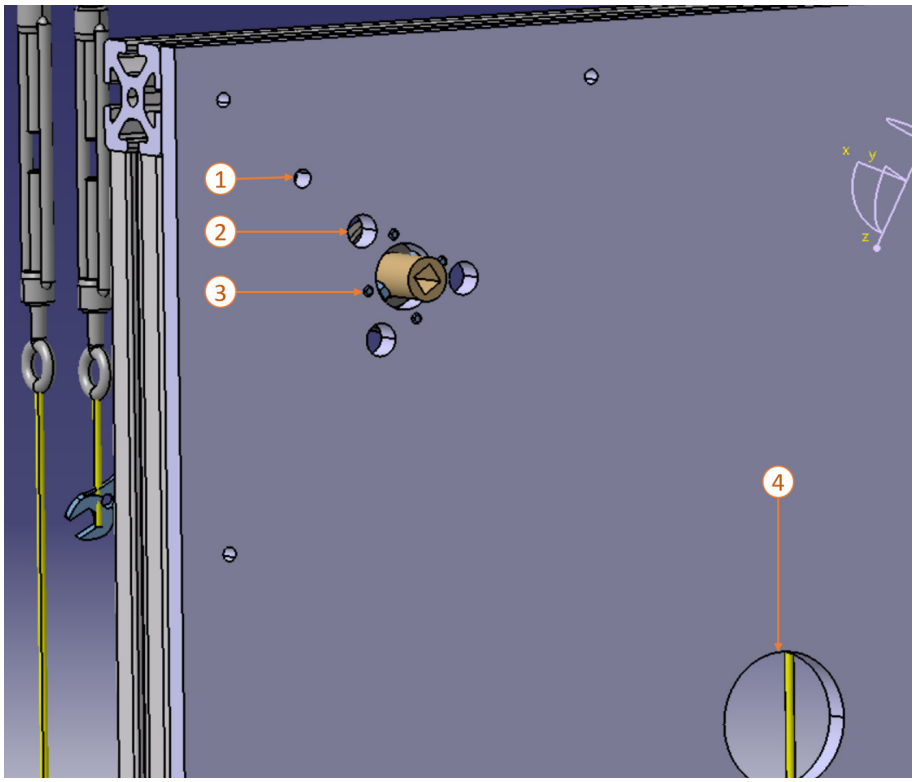

Figure 12: One quarter of the spacecraft simulator plate. With the MECSS/MMX spacecraft holes (1), cup-cone access holes (2), M4 holes for the attachment of the bearing (3), and the centered cutout for the push-off spring shell (4).

The main component of the assembly is the plate itself. It is specially designed and milled for this. As already mentioned in the previous paragraph, the DLR site in Bremen has no real milling capabilities especially not for manufacturing such a large component. Therefore, manufacturing is contracted to an external company. In the past, the department has often worked with the manufacturer 247TailorSteel due to its fast delivery time and sufficient quality for this purpose. The plate is 530 mm in height and 500 mm in width. A laser cutting process that allows a maximum thickness of 10 mm is used for manufacturing. This maximum thickness was chosen to ensure that the plate can transmit in-plane forces caused by the separation without much warping. To enhance stiffness even further, a frame made of aluminum profiles is attached to the edges of the plate. These profiles are also used to attach the structure that has MECSS and PAC mounted to it to the WCI. The plate has a cutout at the middle, to leave enough space for the back of the POM spring shell. Near the corners, there are four additional cutouts where the lever interface assemblies are placed and screwed onto the plate by four M4x20 screws, listed in Table 3.2. Prior to this, the M4 thread (3) must be cut, because the laser cutting procedure used by the manufacturer can only achieve core holes of 3.3 mm.

The three slightly bigger holes concentrically aligned around the bearing exist in case access to the bolted connection of the cup-cone interfaces is needed while the plate is mounted. The outermost four holes in the corners as shown in Figure 12 are needed to fasten the MECSS to the spacecraft simulator plate. More information is given in the integration procedure during the separation tests in Chapter 6.2.

Connecting Beam

The previous paragraph deals with assembly of the spacecraft simulator plate and the integration of the lever interface assemblies into it. Now all of the four ratchet wrenches of each lever interface assembly must be combined into one cable in order to trigger all four HDRMs simultaneously. How this is done is described in the following.

Pos.	Name	Distributor	Dimension	Qty.
1	Profil 8 80x40	Item	$L = 420\,\text{mm}$	1
2	Extension spring	Febrotec	$L_0 = 63.4\,\text{mm}$ $c = 4.86\,\frac{\text{N}}{\text{mm}}$	4
3	Steel cable	Drahtseile24.de	$L = 8000\,\text{mm}$	1
4	DIN 5299 grade C snap hook	Drahtseile24.de	11x120 mm	1
5	DIN 741 clamps	Drahtseile24.de	$D = 4\,\text{mm}$	63
6	Clamp stopper	Drahtseile24.de	$D = 4\,\text{mm}$	1
7	DIN 1480 turnbuckle	Würth	M6	4
8	Hook (WCI)		M6	4

Table 3.4: Parts list of the connection beam assembly.

The ratchet wrenches used in this setup only have one ratchet-end which is attached to the shaft. At the other end the wrench has an open-end. In order to be able to attach a steel cable to the open-end of the wrench a hole just large enough for the steel cable to fit through must first be made. To fix the steel cable, it is put through the hole and fixed with the wire clamp to form a loop. According to the clamp's data sheet, at least three clamps are required per loop to withstand the occurring loads. It must be ensured that the clamping jaw is always on the side of the stressed cable. The length of the cables is almost arbitrary. However, the relative length of the cables is important. The difference between the longer cables for the two lower wrenches and those for the two upper ones must be exactly 355 mm. This ensures that the angles of all wrenches do not differ and thus, the required release force is similar. To ensure that there is sufficient space for the release path, the shorter cables should not exceed 80 mm in length.

As shown in Figure 10, the other end of the cable is attached to a turnbuckle which is connected in series with a spring. The turnbuckle is used to compensate for the small irregularities in the preload. Thus, all cables are pretensioned with the same force. This process is also described in more detail in Chapter 6.2. Due to the spring deflection, the tension present in the cable can be derived easily. The cables can thus be pretensioned so that they are loaded just under the necessary release force. This allows a faster release of the HDRMs. The ends of the springs are latched into hooks which in turn are screwed to the connecting beam. These hooks are already used in the thermal vacuum test campaign and can therefore be adopted just like the basic structure of the WCI. The connecting beam is used to transfer the load from the four cables of the HDRMs to one single cable without changing neither the distances nor angles between those four. The hooks are attached on the lower side of the beam. On the top side, there are four additional attachment points where further cables are mounted. These cables must all have the same length around 200 mm. At each end, there are loops as they have been mentioned before. Each loop is fixed to the connecting beam using a screw with washer. It is important that the loop of the cable is just large enough for the screw to fit through, but small enough that it cannot slip over the washer. The loose end loops are placed all together in the snap hook, also listed in Table 3.4. The 120 mm wide end of the snap hook ensures that the cables keep the same distance and thus the load distribution is also the same. Additionally, placing the cables in a certain order can help. At the narrower end of the snap hook, a single cable runs towards the upper pulley, which is part of the WCI adjustments. These are described in the next Chapter 3.2.2.

3.2.2 Adjustments to the WCI

The separation tests will not be the first separation of MECSS and PAC. During the preceding thermal vacuum tests, the separation is already being tested at least once. In order to be able to perform the separation under space conditions inside the vacuum chamber, the WCI is used. This MGSE provides a solid foundation on which to build the MGSE for the separation tests.

The WCI is assembled from aluminum profiles. The basic structure consists of four, upright 100 mm profiles, which are connected at the top and sides with horizontal profiles to give stability to the construction. Additional profiles were attached to this structure in order to perform the separation inside the chamber during thermal vacuum test. They are no longer needed for the separation tests and were removed in the first step.

The following parts which can be seen in Figure 13 will be dismantled:

- inner profiles, that help with the attachment (1)
- side profile with the pulley (2)
- catching structure for the compensation weight (3)
- trolley on the middle top profile (4)

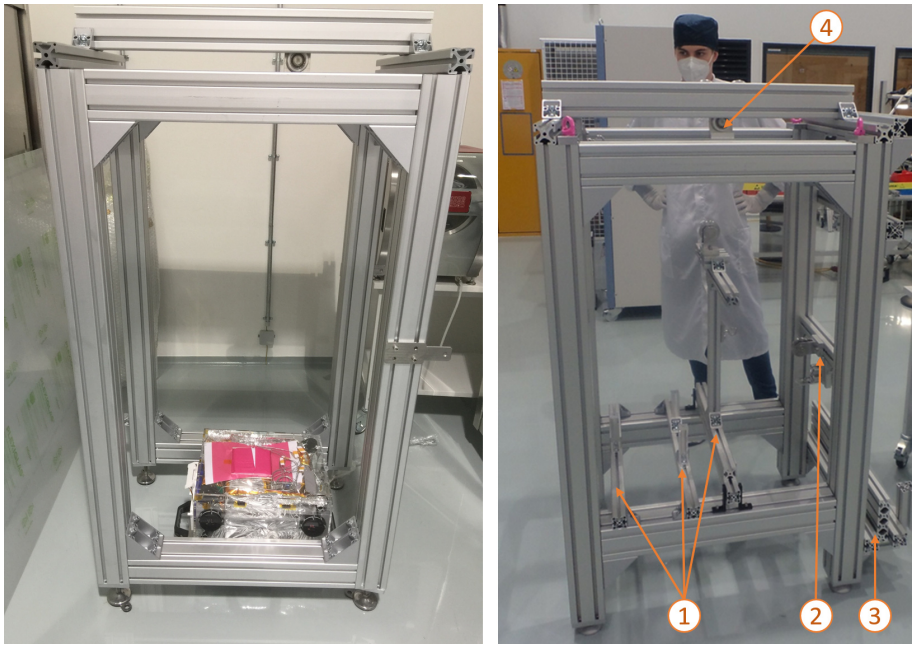

Figure 13: Basic structure of the WCI (left) and the configuration for thermal vacuum test (right).

While the separation in the thermal vacuum test takes place within the four pillars, there is no space for it in terms of the separation tests. Thus, the test object consisting of MECSS and PAC is attached on the outside of the MGSE as already described in the previous Chapter 3.2.1. This leaves space for the trigger support structure as well as a free separation path for the PAC.

After removing the parts that were necessary for the thermal vacuum test, it is time to start attaching the required parts for the external trigger mechanism. In Chapter 3.2.1, the external trigger components are explained. This chapter is about the adjustments of the WCI as well as the attachment of the external parts onto the WCI. In addition, this chapter also describes how the mechanism is triggered by the drop weight.

A single cable leads from the connecting beam up to the pulley at the top edge of the WCI. This pulley has a diameter of 75 mm and a maximal static load capacity

of 600 kg. The ball bearing version of the pulley is used, which can support a cable thickness of 3-8 mm. It is mounted on two 40x40 mm aluminum profiles, so that the pulley extends slightly over the edge and thus the cable does not collide with the structure. These profiles are also used for suspending the drop weight. The suspension of the drop weight is described later in this chapter. The pulley redirects the cable 90 degrees in a horizontal orientation to the second pulley. This second pulley (3) is mounted on the side of the upper profile (2), as shown in Figure 14. The profile already exists in the thermal vacuum test configuration of the WCI, as can be seen in Figure 13. Unlike the thermal vacuum test, the direction of the load during separation tests is not only vertical, but also horizontal in the direction of the angle brackets. Therefore, the connection from the profile (2) to the structure must be strengthened. To ensure this additional margin against displacement of the profile, the 40x40 mm angle brackets securing the beam to the structure are replaced with the larger 80x80 mm angle brackets (1). The cable is then redirected downwards by the second pulley (3), through the two profiles (4) to which the first pulley is attached to.

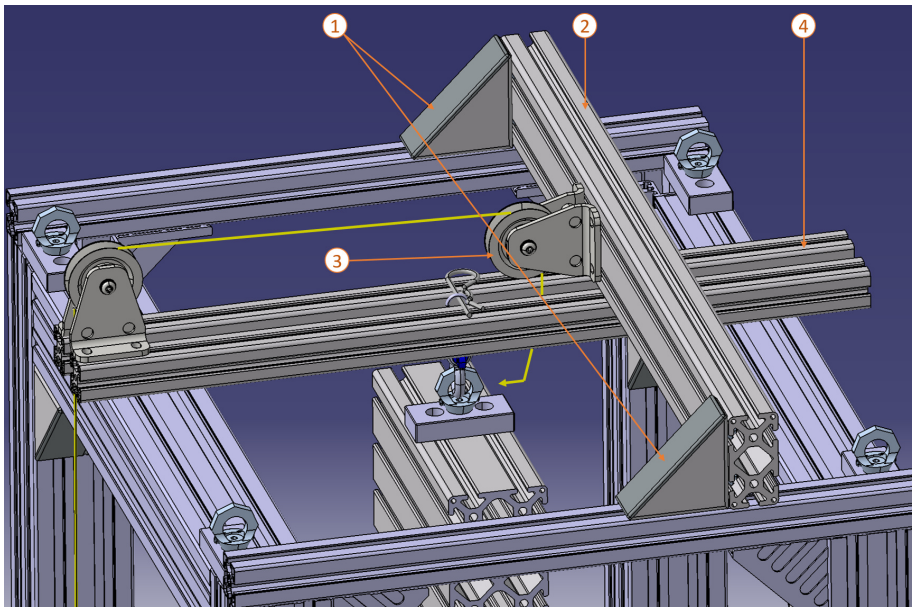

Figure 14: Upper section of the WCI with two 80x80 mm angle brackets (1), the upper profile (2) with the pulley (3) attached as well as the two profiles (4) for the pulley and weight suspension.

As shown in Figure 15, the cable then runs through a 60x16 mm aluminum profile in which a small, centered hole has already been drilled, just large enough for the cable to fit through. A clamp stopper is then placed on the other side of the hole to prevent the rope from slipping through. This allows the rope to be pretensioned to a certain degree in the area from the clamp stopper to the HDRM by using the turnbuckles. Pretensioning is useful because it requires less energy and thus, time during the

triggering process to cause the elastic deformation of the individual components. Since keeping the trigger process as short as possible, this step is particularly helpful because the kinetic energy of the drop weight is transferred almost exclusively to the actuation torque for the HDRMs since the elastic deformation of the individual components like the steel cables turnbuckles or part of the springs is already present. The clamp stopper was also chosen because the length of the cable can be adjusted at any time, whereas a fixed length with loops at each end has very limited possibilities to adapt if changes in length or pretension should be necessary.

The steel cable is another 800 mm long before connected to the drop weight. In addition, the cable should be left a little longer in order to still be able to change the height, which might be necessary in the future. The loop of the steel cable's end is hung into a shackle. This shackle, as shown in Figure 15 is connected to the eyelet, which is attached to the weight. Four of those eyelets are already part of the WCI. At each upper corner, there is one to serve as an anchoring point for the use of a crane. These points are not needed during the test campaign, thus can be used elsewhere. It allows one of them to be moved, as shown in Figure 14. The use of a shackle as an intermediate link aids in removing the weight quickly and thus simplifies the work between tests. In addition, another cable loop is attached to the shackle as well as slid between the two smaller aluminum profiles and fixed with a cotter pin. The drop weight can then be released by pulling the cotter pin. The weight is in free fall for approximately 800 mm before pulling on the steel cable and triggering the mechanism. Due to the preceding acceleration caused by the free fall, the release path of the HDRM is passed quickly, so the separation is triggered as fast as possible, keeping the delay between each mechanism to a minimum. As shown in Figure 15, additional brackets should be placed to the left and right of the cotter pin to ensure that the pin is pulled in a controlled and guided manner.

3.2.3 Attachment of the External Trigger

The external trigger has already been described in Chapter 3.2.1. Now it must be attached to the WCI. This requires the parts listed in Table 3.5.

The PAC is additionally attached with four points to a rope pendulum. The ceiling structure with the rope pendulum can be seen in Figure 20. How exactly the ropes are arranged and where they are attached to the PAC can be found in Chapter 6.4.2. At first, the only important thing is that the ropes must be as long as possible. Since the ropes are rigidly fixed at the top of the ceiling mount, they do not follow the separation path of the PAC. Viewed from the side, the separation path makes a slight upward curve. The longer the ropes, the larger the radius of this curve and thus,

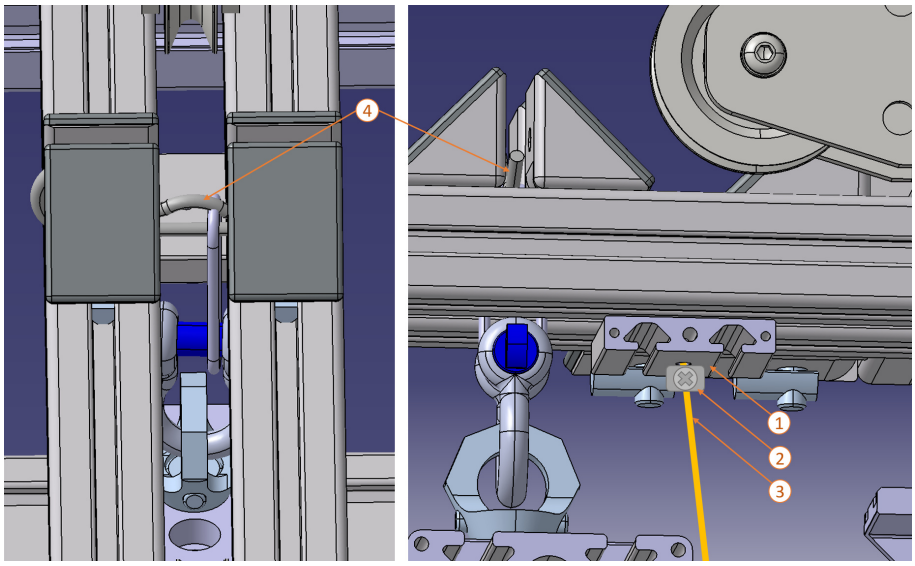

Figure 15: Close-up view on the drop weight release section of the WCI with the Profile 6 60x12 (1), the clamp stopper (2), cable to the drop weight, as well as the release cotter pin (4).

Pos.	**Name**	**Mfr.**	**Dimension**	**Qty.**
1	Profile 8 40x40	Item	$L = 240\,\text{mm}$	2
2	Profile 8 40x40	Item	$L = 800...900\,\text{mm}$	2
3	Angle bracket set 8	Item	40 x 40 mm	18
4	Angle bracket set 10	Item	100 x 100 mm	2
5	Profile 6 60x12	Item	$L = 50\,\text{mm}$	1
6	Shackle GN 585-10-A	Ganter Norm	$ID = 26\,\text{mm}$	1
7	Steel pulley w/ ball bearing	Frank-seilrollen.de	$D = 75\,\text{mm}$	2

Table 3.5: Parts list of the WCI adjustments, as well as for the attachment of the external trigger (Pos. 1-3).

the smaller the vertical translation of the PAC. Therefore, the distance between the edge of the spacecraft simulator plate and the floor is set to 110 mm. This leaves enough space for the wrenches to rotate, and between PAC and floor during separation. Approximately 90 mm from the bottom edge of the spacecraft simulator plate, just above the long versions of the lever interface assembly, an aluminum profile is attached to the frame of the simulator plate with two angle brackets. The two shorter aluminum profiles from Table 3.5 are placed to the side of the upper edge of the simulator plate frame and fixed with two bracket angles, as shown in Figure 16. While the lower profile carries the main load, the upper profiles primarily prevent the tilting caused by the weight induced momentum.

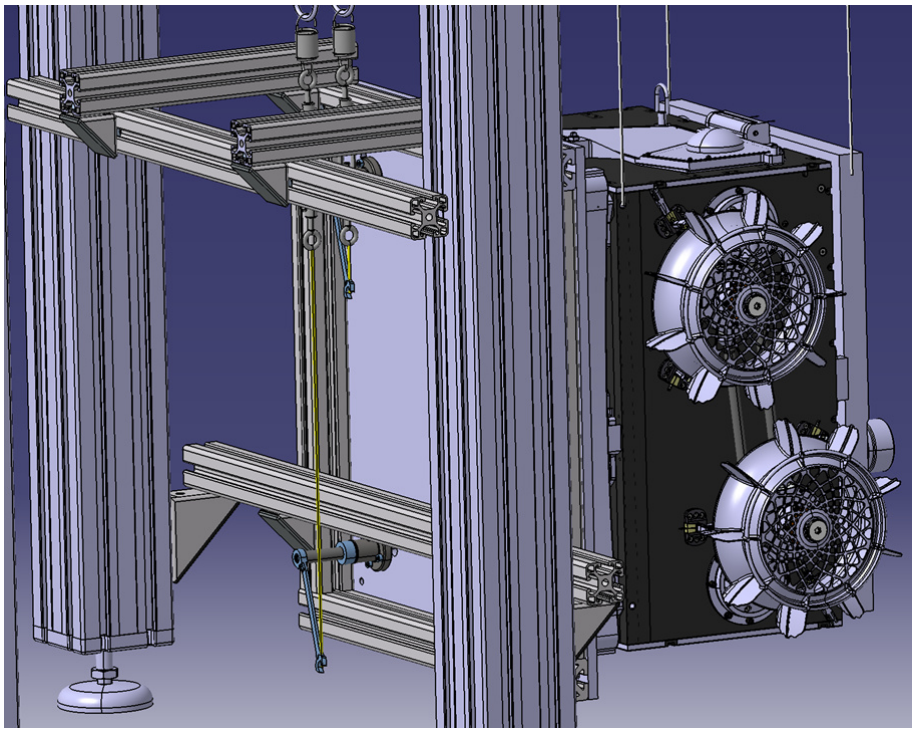

Figure 16: Detailed view of the connection between spacecraft simulator plate and WCI.

4 Calculations

4.1 Determination of the Required Torque

The HDRMs used in the separation tests require a torque to release. This Torque is applied by a wrench, which is rotated by a drop weight. To calculate the required mass for the drop weight, the needed release torque must be determined in the first place. First of all, the HDRM is preloaded in exactly the same way as the flight version. Chapter 1.3.1 already touches on the subject and Figure 6 shows various steps of the flight version HDRM during this process.

To preload the Mechanism, the special apparatus as shown in Figure 17 below is used. This is screwed onto the threaded rod compressing the spring together with the upper cap. By tightening the brass-colored nut on top, the spring inside the cup-cone interface is compressed. The cable leading out of the casing is plugged into a computer, where the load of the bolt can be displayed.

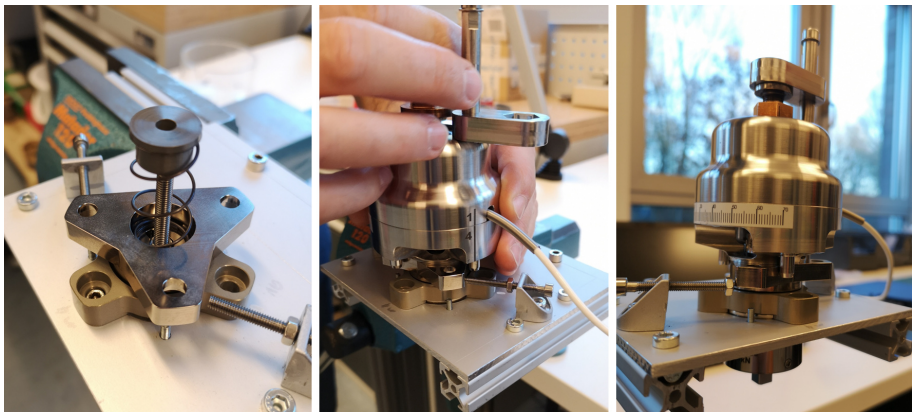

Figure 17: Reusable version of the Glenair HDRM 061-005 during the preload.

Another nut between the spring cap and the clamping device is hand-tightened. This keeps the spring compressed after the equipment has been removed. In order for the device to determine the correct force on the spring, the load must be exclusively on the nut of the device. This creates the problem that the actual load of the other, permanent nut cannot be accurately measured with this apparatus. Therefore it was determined experimentally by how many degrees the nut must additionally be tightened to achieve the required preload of 13 kN.

Once the HDRM is preloaded, it was able to start determining the required torque for triggering. Therefore, the mechanism remained screwed to the support plate as

shown in Figure 17. Then, the plate with the mechanism was rotated 180 degrees so that the release interface faces up and the retaining bolt faces down. This allows a small amount of force to be applied to the retaining bolt in order to better identify when the mechanism releases the bolt. A torque wrench with a wrench size 8 attachment was used to turn the rectangular interface of the HDRM. Although it has a pointer that indicates the maximum measured torque, the torque was closely observed at all times. The maximum torque during this test got close to 5 Nm, but never exceeded this value. Therefore, 5 Nm was used as reference for further work. As soon as the holding force was overcome, the required torque dropped to 3-4 Nm. This value is also used as a reference for later calculations.

In addition, the tests have confirmed that no specific trigger point can be identified. Therefore, it is essential to complete the 90 degree release path as quickly as possible in order to keep the delay between the HDRMs to a minimum.

4.2 Dimensioning of the Springs

After the release torque was determined, the corresponding release force is calculated. To do so, the relation between torque T, force F and lever arm r is needed:

$$T = F \cdot r \tag{4.1}$$

The projected lever arm depends on α, thus $r(\alpha)$. Due to the varying angle over the release path, the required force also changes. In order to keep the required force as small as possible, the path is described symmetrically with respect to the horizontal as follows:

$$-45^\circ \leq \alpha \leq +45^\circ \tag{4.2}$$

Due to the ratchet wrench's minimum adjustment angle of 5°, this value can be set quite accurately. Thus, a starting angle of 45° is assumed for this calculation.

First, the cosine is used to calculate the projected lever arm at the starting angle of -45°. With the real length of the wrench of 126 mm as hypotenuse and the chosen angle of 45° follows:

$$r(\alpha = 45^\circ) = 126\,\text{mm} \cdot \frac{1\,\text{m}}{1000\,\text{mm}} \cdot cos(45^\circ) = 0.089\,\text{m} \tag{4.3}$$

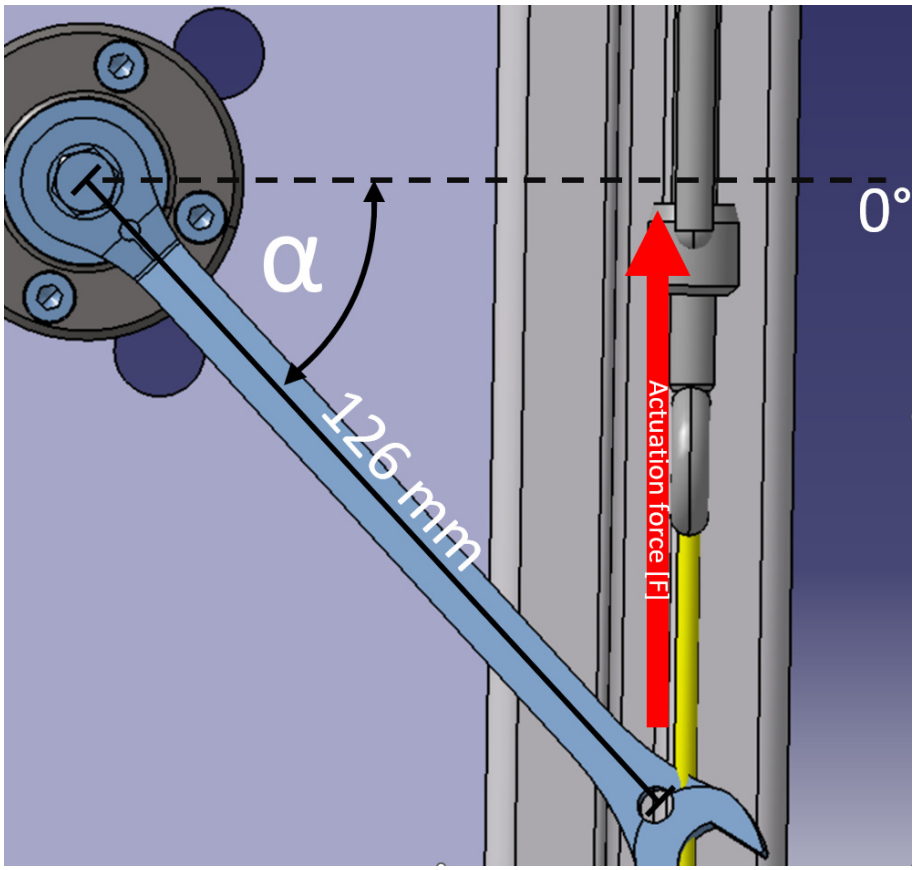

Figure 18: Definitions of lengths and angles.

Inserting 4.3 into 4.1 and transposing to F, gives:

$$F_{req} = F = \frac{T}{r} = \frac{5\,\text{Nm}}{0.089\,\text{m}} = 56.12\,\text{N} \tag{4.4}$$

When the weight starts pulling on the cable, the springs extend until the release force is reached. Then, the wrenches begin to move and the mechanisms are triggered. Later in Chapter 6.4.1 it is shown that the required force decreases after the holding force has been overcome and the ratchet wrench is moving. Additionally, the angle α shown in Figure 18 first decreases which also results in a reduction of the required force. However, after the wrench passes the horizontal position, the angle also increases again.

Based on this calculation, the spring with the designation '0E0750-0952500S' from Febrotec was selected as suitable. With its compact length $L_0 = 63.4\,\text{mm}$, it fits well into the setup. Its spring constant c of $4.86\,\text{N/mm}$ provides sufficient stiffness to transmit the necessary forces. The deflection of the spring will also be measured to determine the preload force mentioned in Chapter 6.4.1. Therefore, it is important that the change in length for the occurring forces can be measured precisely. With

a test length of 91.95 mm and the associated force of 152.74 N, it ensures a safety factor of almost three.

4.3 Dimensioning of the Steel Cable

The rope will experience a shock as the weight falls into the steel cable. The power of this shock and the resulting necessary strength of the cable is determined in the following. Since the load is dynamic and depends on many small factors, an exact calculation can only be made using numerical methods. For this reason simplifications are made in this calculation so that the magnitude of the occurring forces is still accurate. Nevertheless, in this case a very exact calculation is not necessary at all since the maximum allowed load of the cable varies strongly with the diameter. In order to further increase safety, a larger diameter should be selected when possible.

The real structure must be transferred into a substitute model. For this, it can be broken down as follows. First, all masses between the drop weight and the spring are combined into one mass:

$$m_{tot} = m_{cable} + 4 \cdot m_{hook} + m_{beam} + m_{carabiner} \tag{4.5}$$

For the mass of the cable it is first assumed that the diameter is 4 mm. According to the manufacturer, the mass of the cable is 55 grams per meter. Adding up all the lengths results in a total cable length of 2.35 m. It should be mentioned here that the last 0.8 m of the cable up to the drop weight is only partially accelerated by the pull of the drop weight. The end of the cable at the drop weight will have the same speed at the end of the free fall as the drop weight. The upper end will remain stationary until the weight pulls. In between, a simplified linear acceleration can be assumed which would further reduce the mass that needs to be accelerated. However, as will be seen in 4.8, the mass of this 0.8 m cable is much smaller than the total mass of the cable (with its clamps), thus a reduction is not applied. This is legitimate since this reduction would only result in a reduced load on the cable. In addition, there are 27 DIN 751 clamps for the loops, each weighing 13 grams. All partial masses of the cable result:

$$m_{cable} = 2.35\,\mathrm{m} \cdot 0.055\,\frac{\mathrm{kg}}{\mathrm{m}} + 27 \cdot 0.013\,\mathrm{kg} = 0.48\,\mathrm{kg} \tag{4.6}$$

With the other masses inserted into equation 4.5 gives:

$$m_{tot} = 0.48\,\mathrm{kg} + 4 \cdot 0.083\,\mathrm{kg} + 0.458\,\mathrm{kg} + 0.180\,\mathrm{kg} = 1.450\,\mathrm{kg} \tag{4.7}$$

Here is why neglecting the weight reduction of the last 0.8 m of the cable is valid:

$$0.8\,\mathrm{m} \cdot 0.055\,\frac{\mathrm{kg}}{\mathrm{m}} << 1.450\,\mathrm{kg} \tag{4.8}$$

The next step is to calculate the weight's velocity just before the cable is tightened by it, thus the acceleration of the drop weight equals the gravitational acceleration g.

$$g = 9.81\,\frac{\mathrm{m}}{\mathrm{s}^2} \tag{4.9}$$

Integrating this equation with respect to time gives:

$$v(t) = gt \tag{4.10}$$

Integrating this equation - again - with respect to time results in:

$$s(t) = \frac{1}{2}\,gt^2 \tag{4.11}$$

To calculate the final velocity of the weight, the duration of the fall must first be determined. The drop distance s is known to be 0.8 m. Equation 4.11 resolved with respect to t results in:

$$t = \sqrt{\frac{s}{\frac{1}{2}\cdot g}} = \sqrt{\frac{0.8\,\mathrm{m}}{\frac{1}{2}\cdot 9.81\,\frac{\mathrm{m}}{\mathrm{s}^2}}} = 0.4039\,\mathrm{s} \tag{4.12}$$

Inserting t into Equation 4.10 gives the velocity of the weight just before it pulls on the cable.

$$v(0.4039\,\mathrm{s}) = 9.81\,\frac{\mathrm{m}}{\mathrm{s}^2}\cdot 0.4039\,\mathrm{s} = 3.9618\,\frac{\mathrm{m}}{\mathrm{s}} \tag{4.13}$$

In Chapter 4.2, Equation 4.4 already determined the required actuation force. This force must be multiplied by four to get the total release force of all HDRMs.

$$F_{ges} = 4 \cdot F_{req} = 4 \cdot 56.12\,\mathrm{N} = 224.48\,\mathrm{N} \tag{4.14}$$

In addition, the springs need to be summarized. Since this is a parallel configuration, all spring stiffnesses can be summed up. This results in the following:

$$c_{ges} = 4 \cdot c = 4 \cdot 4.86\,\frac{\mathrm{N}}{\mathrm{mm}} = 19.44\,\frac{\mathrm{N}}{\mathrm{mm}} \tag{4.15}$$

The weight now pulls on the cable and stretches all components between turnbuckle and weight. Due to the preload mentioned in Chapter 6.4.1, a certain elastic deformation is already present so that - simplified - only the spring experiences an elastic deformation. This assumption is very conservative and any neglected spring effect such as that of the cable would only reduce the maximum load occurring in the cable. Therefore, this includes additional safety. The weight as described in more detail in Chapter 4.4 is much heavier than the mass to be accelerated from Equation 4.7. Therefore, the weight can be simplified by assuming that it continues to fall without deceleration while the masses in the external trigger are accelerated.

Simplified, one can say that the masses are accelerated until the necessary actuation force is reached due to the spring deflection.

The deflection of the spring can be calculated with this equation:

$$F = c \cdot \Delta l \tag{4.16}$$

With F_{ges} from Equation 4.14, c_{ges} from Equation 4.15 and transposed to Δl gives:

$$\Delta l = \frac{F}{c} = \frac{224.48\,\mathrm{N}}{19.44\,\frac{\mathrm{N}}{\mathrm{mm}}} = 11.55\,\mathrm{mm} \tag{4.17}$$

To determine the maximum force occurring in the cable, the following formula is used:

$$F_{cable} = m_{tot} \cdot a \tag{4.18}$$

The force in the cable depends on the mass m that must be accelerated by the drop weight. In addition, the acceleration rate a of it is needed. The acceleration can be calculated using Equation 4.11. Therefore, $g = a$ and distance s equals spring deflection Δl. Transposed to a gives:

$$a = \frac{\Delta l \cdot \frac{1\,\mathrm{m}}{1000\,\mathrm{mm}}}{0.5 \cdot t^2} \tag{4.19}$$

Since the mass of the drop weight is much greater than the mass to be accelerated it can be simplified by assuming that the weight continues to fall without deceleration after pulling on the cable. This assumption is conservative; in reality, the deceleration of the weight results in a reduced load in the cable. With the spring deflection from Equation 4.17 and the velocity v from Equation 4.13 the time required to calculate the acceleration in Equation 4.19 can be determined.

$$t = \frac{\Delta l}{v} = \frac{11.55\,\mathrm{mm} \cdot \frac{1\,\mathrm{m}}{1000\,\mathrm{mm}}}{3.9618\,\frac{\mathrm{m}}{\mathrm{s}}} = 0.0029\,\mathrm{s} \tag{4.20}$$

This inserted into Equation 4.19 gives:

$$a = \frac{\Delta l}{0.5 \cdot t^2} = \frac{11.55\,\mathrm{mm} \cdot \frac{1\,\mathrm{m}}{1000\,\mathrm{mm}}}{0.5 \cdot (0.0029\,\mathrm{s})^2} = 2718.57\,\frac{\mathrm{m}}{\mathrm{s}^2} \tag{4.21}$$

This a and $m_{tot} = 1.449\,\mathrm{kg}$ from Equation 4.7, inserted into Equation 4.18 gives:

$$F_{cable} = m_{tot} \cdot a = 1.449\,\mathrm{kg} \cdot 2718.57\,\frac{\mathrm{m}}{\mathrm{s}^2} = 3939.2\,\mathrm{N} \tag{4.22}$$

According to the steel cable's data sheet, for the 4 mm cable a maximum load of $F_{Cmax} = 13\,200\,\mathrm{N}$ is allowed. The factor of safety S is thus:

$$S = \frac{F_{Cmax}}{F_{cable}} = \frac{13\,200\,\mathrm{N}}{3939.2\,\mathrm{N}} = 3.35 \tag{4.23}$$

A sufficient factor of safety is therefore present. With a 5 mm cable, the factor could be increased to >5.

4.4 Dimensioning of the Drop Weight

In order to estimate the magnitude of the drop weight, the minimum required weight must first be calculated. The required initial release force per HDRM was calculated in Equation 4.4 and summarized in Equation 4.14 to $F_{req} = 224.48\,\mathrm{N}$. Once the wrench is in motion, the required torque reduces to 3.5 Nm, resulting in $F_{req} = 157.12\,\mathrm{N}$. Since the weight falls into the rope and thus has an impulse, the lower required torque can be used for calculation because it can be assumed that the momentum will overcome the holding torque of 5 Nm.
The friction of the pulleys can be neglected since F_{req} is orders of magnitude greater. The mass required to achieve the force F_{req} can be determined by rearranging Equation 4.18 as follows:

$$m_{trigg} = \frac{F_{req}}{g} = \frac{157.12\,\mathrm{N}}{9.81\,\frac{\mathrm{m}}{\mathrm{s}^2}} = 16.02\,\mathrm{kg} \tag{4.24}$$

Additional weight is needed to compensate for the mass of cables, connecting beams, and all other components between the weight and the HDRCs. This mass calculated in Equation 4.7.

$$m_{add} = m_{tot} = 1.449\,\mathrm{kg} \tag{4.25}$$

Thus, the following mass is required to trigger the HDRCs.

$$m_{weight} = m_{trigg} + m_{add} = 16.02\,\mathrm{kg} + 1.449\,\mathrm{kg} = 17.469\,\mathrm{kg} \tag{4.26}$$

It also shows that the simplification that the falling weight is not slowed down by the acceleration of m_{tot} is valid, because:

$$m_{weight} >> m_{tot}$$
$$17.469\,\mathrm{kg} >> 1.449\,\mathrm{kg}$$

Due to the inertia of the drop weight already mentioned above, the weight can most likely be reduced further. With decreasing mass, the assumption that the falling weight is not slowed down - even while it is pulling on the cable - becomes invalid. Experiments must be carried out to determine when deceleration of the weight has a negative effect on the duration of the release procedure. A weight as small as possible should be used in order to protect the equipment and also to minimize the interference in the measurements that a heavy drop weight may cause.

5 Implementation

Initially, this chapter should be a complete documentation of the implementation. As it has been made clear several times in the concept, the WCI is a essential part of the setup. However, it is still needed in the preceding thermal vacuum tests. The WCI is already prepared for these tests, so it was not available even though the thermal vacuum test will not start before October 2022.

Originally, the separation tests were scheduled for spring 2022. Due to an incident in an early vibration test, which required a change in the design, the all following tests were postponed. That means that testing will be resumed after the publication of this thesis. Meaning that the test campaign will start again - with the updated SM2 - later in the year after the submission of this thesis. Thus, the implementation could not be documented here in more detail. To avoid further delays in the schedule all necessary purchase orders have already been placed or even arrived. This means that implementation can begin immediately after thermal vacuum tests have been completed. This is currently expected to happen in October/November 2022. Furthermore, as mentioned in Chapter 4.1, the reusable version of the HDRC was analyzed on its behavior and the findings were implemented in the concept.

6 Test Specification

6.1 Test Setup Environment

This Chapter is about the whole test setup. It includes the preparation of the test environment as well as the enumeration and explanation of the measuring instruments used.

6.2 Preparation of the Test Stand

The separation tests will take place in the Landing and Exploration Technology (LET) laboratory at the DLR site in Bremen. It already exists a support structure, which was developed for MASCOT follow-on technology tests, which is attached to the ceiling of the laboratory. From this structure, the PAC is suspended with four ropes. This allows it to move freely after separation from the MECSS.

A general overview of the test setup in the LET laboratory can be seen in Figure 19 below.

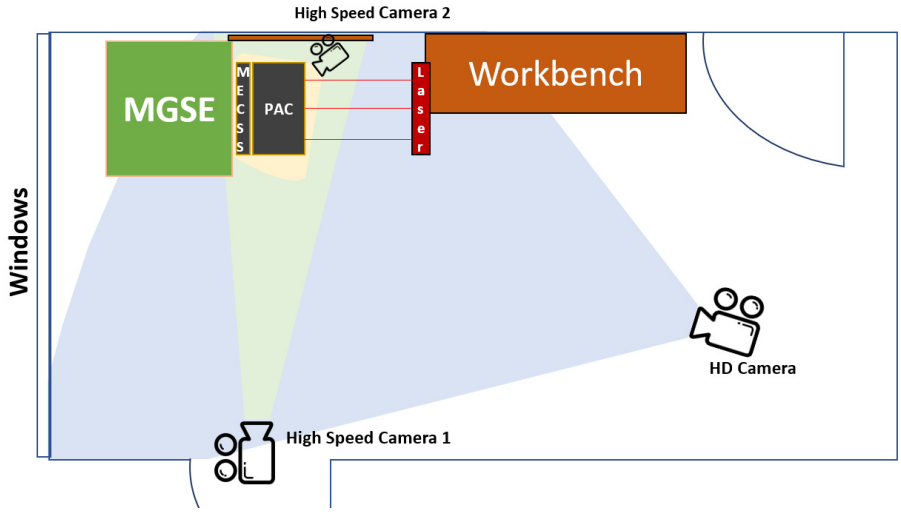

Figure 19: Sketch of the test setup at LET Laboratory.

First, the MGSE is placed under the ceiling structure. It should be placed a little further towards the windows so that the ropes are almost orthogonal to the PAC, which will be mounted later. Thus, the horizontal separation path is maximized before the vertical error becomes a problem. The ceiling structure is shown in

Figure 20. The spacing of the four ropes shown in the right part of the figure can be adjusted by moving or exchanging the aluminum profiles.

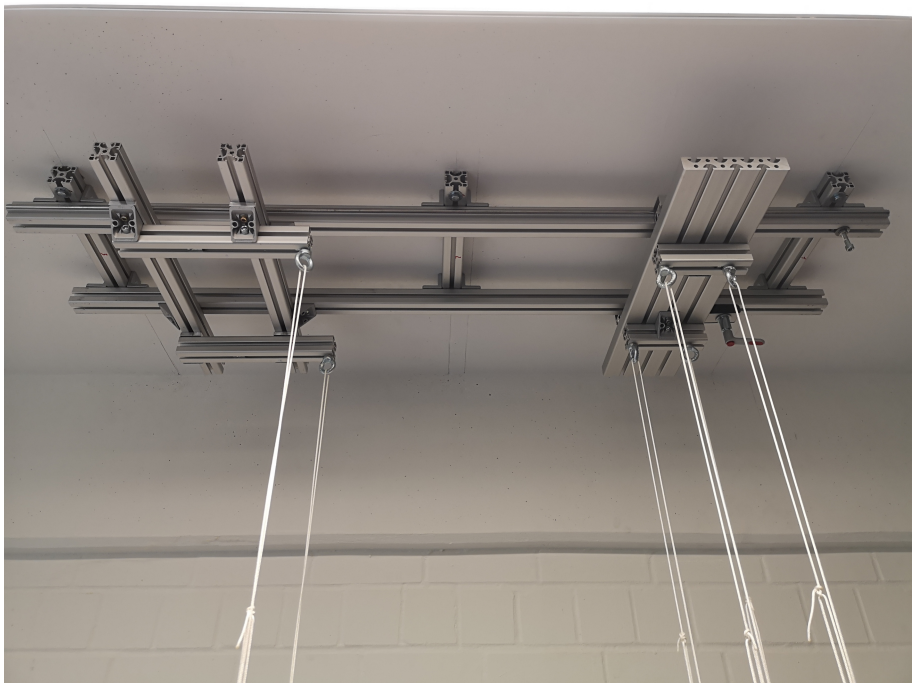

Figure 20: Ceiling mounting structure at LET Laboratory.

Furthermore, a wall is put behind the separation path of the PAC. This wall with chessboard-like pattern, can provide important references on the high speed camera's footage. For example, to determine the separation velocity. The High Speed Camera 1 requires some distance and may therefore be placed in the door frame. It is important to ensure that the environment to be captured is sufficiently illuminated. The higher the frame rate, the more light is required since the exposure time per frame decreases with an increasing frame rate. LED spotlights cannot be used as they have a certain flickering effect, which is disturbing on high speed footage. Therefore, construction spotlights with halogen bulbs are used since they are more resistant to mains frequency of 50 Hz. The High Speed Camera 2 can either be mounted on the ceiling structure or directly onto the WCI. The HD Camera is mounted on a tripod to capture the entire test environment.

In addition, the three laser measuring devices must be brought into position, as described in Chapter 6.3. The various sensors must then be connected to the Data Acquisition (DAQ) system and configured via the corresponding computer on the workbench. Two additional computers are needed, which are also listed in Table 6.1. The following Chapter 6.3 describes the measuring instruments and methods used in the separation tests.

6.3 Measurement Instruments and Methods Used

Main purpose of the separation tests is the qualification of the separation mechanism. The results provide information about the behavior during regular separation without problems as well as in special cases of abnormal performance. Such data is necessary to verify if the separation process works properly and the separation corridor defined by JAXA is respected. Many different instruments are used in order to receive those data.

An overview can be seen in this Table 6.1.

Name	**Type**	**Data Rate**	**DAQ**	**Program**
High Speed Camera 1	Fastcam SA3	1000-2000 FPS	PC-1	Fastcam Viewer
High Speed Camera 2	Casio Exilim EX-F1	300 FPS	SD Card 1	-
HD Camera	EOS-650D	30 FPS	SD Card 2	-
Accelerometer (1 Axis) (4pcs)	PCB 35003B03	2400-4800 Hz	MX840A MX1601 PC-2	Catman Easy
Laser distance sensor (3pcs)	Allsens AM300-500	2400-4800 Hz	MX840A MX1615 PC-2	Catman Easy
Inertial Measurement Unit (IMU) wireless	NG-IMU	400 Hz	PC-3	NG-IMU control

Table 6.1: Measurement instruments for the separation test campaign.

One characteristic that must be observed closely is the trajectory of the PAC. To do this, a laser is used. With a sampling rate of 2.4 kHz, this sensor will measure the distance to the PAC. With this data plotted over time, the velocity can be derived. The laser is placed along the separation axis Z, pointing centered onto the top plate of the PAC. Thus the model moves towards the laser source after separation. In addition, two further laser sensors are used. Placed left and right of the central laser, they will provide additional data to identify possible rotation of the PAC.

At each corner, immediately next to the HDRMs, an accelerometer is attached to the MECSS structure. They provide reliable data for each HDRM if and when it is triggered. For the electrical triggered flight-version, the manufacturer guarantees a triggering within 100 ms when a current of 3.5 A is applied. Because the mechanical

trigger mechanism tends to trigger less accurately than the electrical firing due to the way it works, this information is especially important. A sampling rate of 19 kHz may be required to properly detect the shock, caused by the firing HDRM. All data from the lasers as well as the acceleration sensors are processed in the DAQ system MX840A. This system gathers the measured value over time and due to the central processing, temporal correlations between the sensors can be directly derived. The calibration of the sensors must be checked in the software before running the tests and - if necessary - performed again.

Inside the PAC a Inertial Measurement Unit (IMU) is used. It provides additional data about the orientation and behavior of the PAC. Its data is transmitted via WiFi signal and processed separated from the DAQ system. Thus, the data sets need to be synchronized.

In addition to the measuring instruments just mentioned, three cameras will also be used in the test. One of them being a high speed camera, capable of recording up to 2000 Frames Per Second (FPS). It will be positioned laterally, perpendicular to the separation line (see Figure 19). Due to the highest frame rate of these cameras it is expected that its images will provide significant insight into the separation behavior of the test object.
Another camera observes the tests at a frame rate of 300. The third camera will accompany the tests from a further away bird's eye view. This will give an overview of the complete test environment and document the entire test procedure at a frame rate of 30 FPS.

6.4 Test Procedure

Among others, the scenarios to be tested and the test procedure are covered in this chapter. As soon as the preparations according to Chapter 6.2 have been completed, the actual preparations of the test object can be started.

The steps are as follows:

1. HDRMs are being preloaded (Refer to Chapter 4.1).

2. HDRMs are integrated into the MECSS.

3. MECSS is mated with the PAC.

4. MECSS and PAC are bolted to the spacecraft simulator plate.

5. Spacecraft simulator plate is mounted to the WCI.

6. Springs are hung into the hooks, creating a connection to the drop weight. (Refer to Chapter 6.4.1)

7. Rope pendulums from the ceiling are attached to the PAC (refer to Chapter 6.4.2).

8. Drop weight is secured with the cotter pin at top of the WCI.

9. Cable is hung on the drop weight.

After these steps have been completed, the actual testing can begin. The next step is to check the measuring instruments and cameras for functionality. As soon as all devices are working properly, data acquisition can be started. It should be noted that the high-speed camera also has a high data rate due to the high frame rate. Thus, only a few seconds can be recorded at a time, which is why the start of recording should occur immediately before releasing the drop weight.

After a completed separation, the PAC is removed from the ropes. The springs are also removed from the hooks and the spacecraft simulator plate with the MECSS is detached from the WCI. After that, the MECSS needs to be detached from the plate and the HDRMs removed. Then, another test cycle can be initiated by following the steps of the list above.

6.4.1 Connection and Preload Process

First, the spring hook is hung in the eyelets of the turnbuckle. After passing the connecting beam, the cable is guided over two pulleys, as described in Chapter 3.2.2 before. Once it has passed the last pulley, the cable runs through an aluminum profile and is secured from the other side with a stopper to prevent it from slipping through (refer to Figure 15). This stopper needs to be moved so that the cable is tight and visibly elastic deformed together with the loops. When pretensioning by moving the clamp stopper it is important that the turnbuckles are completely relaxed, means as long as possible. This allows the preload in the spring to be increased sufficiently later by the turnbuckles.

The HDRM is triggered by a torque of 5 Nm. In order to be able to apply this torque, a certain force is required at the end of the wrench, depending on its angle. This force, which is calculated in Chapter 4.2 by a similar calculation, should already

be approximated by the preload but must never be exceeded. In order to ensure this, the cable is only pretensioned so that a maximum of 3.5 Nm is applied to the mechanism.

Inserting 4.3 into 4.1 and transposing to F, gives:

$$F = \frac{T}{r} = \frac{3.5\,\mathrm{Nm}}{0.089\,\mathrm{m}} = 39.28\,\mathrm{N} \tag{6.1}$$

In each cable, a pretension of 39.28 N should be present. This force in the cables can be determined by the deflection of the spring. The correlation between spring force and deflection is described in this equation:

$$F = c \cdot \Delta l \tag{6.2}$$

Since the spring constant c is known from the manufacturer's data sheet with a tolerance of $\pm$ 10 %, the desired force F has been calculated above. The equation can now be transposed to Δl.

$$\Delta l = \frac{F}{c} = \frac{39.28\,\mathrm{N}}{4.86\,\frac{\mathrm{N}}{\mathrm{mm}}} \tag{6.3}$$

The required deflection of the spring is now determined and can be set using the turnbuckles and a vernier caliper.

6.4.2 Rope Pendulums

In Figure 20, the ceiling mounting structure at the LET laboratory is shown. It also shows the ropes (the four on the right) from which the PAC is suspended. There are a total of four M6 threaded holes on the side of the base plate of the PAC. During integration, they serve as an interface for various MGSE. These holes will also be used in the separation test campaign by attaching two of the four rope pendulums there. However, there are no such holes on the top plate to attach the other two rope pendulums. Thus, an interface on the solar array structure model must be created, which is shown in Figure 21 alongside the already mentioned M6 holes.

How exactly the ropes will be attached to the solar array is not sure yet. Basically, there are two concepts. The first concept is to drill a hole in the structural model at the point, also shown in the Figure. This allows a screw to be attached here along with the rope. On the other side, a nut is used for counter-screwing. Thus, a quick mounting and dismounting is also possible. However, this option is only possible if the solar array structure model with those modifications can still be used for the

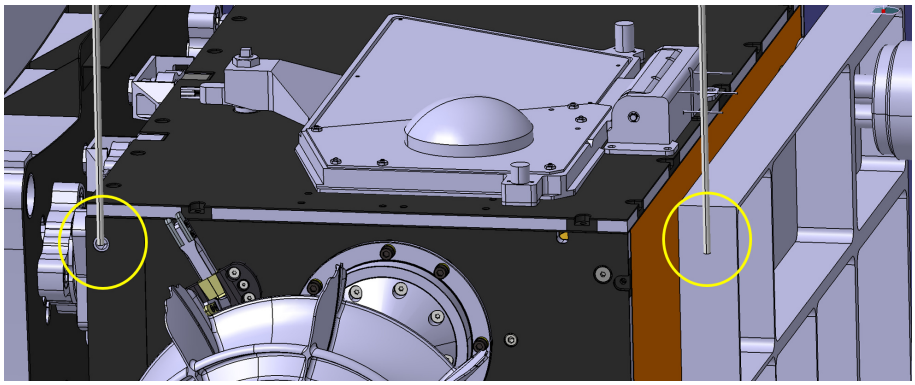

Figure 21: Detailed view of the rope pendulum attachment at the M6 MGSE holes (left) and solar array structure model (right).

remaining tests. Since the separation tests are - as of the publication of this thesis - the last tests for this model, this could be an option to consider.

Another, less invasive option would be to glue a TC-105 to these marked spots. A TC-105 is a small 25x13 mm aluminum plate, with a kind of eyelet that is initially designed for cable ties. These are also used for example in the cable routing of the MECSS. With the two-component glue "Eccobond 285" with hardener "C27" by Henkel Adhesives, a sufficient adhesive connection would be created to use the TC-105 as a rope suspension. A similar solution was already used in the rover's drop tests. Once the tests are completed, it could be removed without residue. However, the preparation of this adhesive connection is somewhat more complex.

In either case, the ropes are attached to the PAC at approximately the same location as shown in Figure 21.

6.5 Test Scenarios

As already briefly mentioned in Chapter 2, the entire separation test campaign will contain many separations. The different cases are divided as follows:

Scenario	Speciality	Amount of Separations 0° / 90°
1	nominal separation; to achieve significant statistic	10 / 10
2	1 s delayed separation; caused by one asynchronous fired HDRM	1 / 1
3	reduced push-of force; caused by the missing spring inside the push-of mechanism	1 / 1
4	reduced push-of force; caused by the not preloaded HDRMs	1 / 1
5	reduced push-of force; caused by the missing pins of the umbilical connector	1 / 1
6	reduced push-of force; caused by the missing bolt pull-out springs	1 / 1
7	Tilted POM	1 / 1
8	delay of one HDRM in order of 50 ms; only if scatter in nominal separations is very small	1 / 1
9	final shot; performing with the flight version electrically fired	at least 1

Table 6.2: All scenarios, tested during the separations test campaign.

A detailed description of these scenarios is given in the following chapters.

6.5.1 Scenario 1: Normal Separation

In order to make correct statements about the reliability of the separation mechanism, several separations are needed. Even if the procedure remains the same, there are certain differences in each separation in terms of separation direction, speed and rotation of the PAC. To ensure that these deviations remain within the given requirements, a sufficiently large number of separations must be done. Since each separation requires a considerable amount of time, a total of 20 normal separations

was chosen. Ten of which are done in the configuration, presented in this thesis. For the other ten separations, the spacecraft simulator plate with the attached MECSS and PAC are rotated by 90 degree around the Z axis to acquire data for the other axis as well. The defined coordinate system is shown in Figure 9. This requirement was already taken into account in the design process of the MGSE and can be implemented without major adjustments. Therefore, it is not described any further.

6.5.2 Scenario 2: Delayed Separation - Redundancy

This and all following scenarios are performed in the initial position as shown exemplary in Figure 9. Chapter 1.3.1 describes how the trigger mechanism of the HDRC works. After the main electrical pulse the wire inside the mechanism should be cut, releasing the retaining bolt. A second pulse - exactly one second after the main pulse - is sent through the redundant circuit and cuts the wire from the other side. This increases the tolerance for errors and ensures correct separation, even if the first electrical pulse is unsuccessful. In this scenario, the separation behavior is tested in this off-nominal case by firing one of the HDRCs with a delay.

6.5.3 Scenario 3: Push-of Spring

The by far largest push-off force is applied by the spring inside the POM, which pushes the rover away by the POP. If the plate or spring has seized or snagged, this force may be reduced or missing entirely. Therefore, when combining the MECSS and the PAC, the POM is omitted and the effects on the separation behavior are investigated.

6.5.4 Scenario 4: HDRM Untensioned

Chapter 4.1 explains the procedure for preloading the HDRMs with a force of 13 kN. The preload ensures that no gapping happens due to the launch loads. The bolts are pulled out by a dedicated spring. Those not working is another off-nominal test scenario, which is listed on sixth position in Table 6.2. This rapid retraction provides another - though small - force that assists the rover's separation from the MMX spacecraft. If the preload is not applied to the mechanism, or the spring inside has lost its load after the cruise phase, this result in a reduced push-off force. The separation behavior in this special case is examined in this scenario.

6.5.5 Scenario 5: Umbilical Connector Pins

The contacts of the umbilical connector are constantly pressing against each other to ensure a continuous power and data connection between rover and MMX spacecraft during cruise phase. This force - like the preload of the HDRMs of Scenario 6.5.4 - plays a minor part in separation. This scenario examines the effects in case those are missing.

6.5.6 Scenario 6: Missing Bolt Pull-Out Springs

The impact on the separation in case the pull out spring of the bolt is missing, is tested in this scenario. The spring as shown in Figure 7 ensures that the bolt is retracted quickly after release. This not only aids separation slightly but also ensures that the released bolt does not collide with any of the spacecraft's structure during separation.

6.5.7 Scenario 7: Tilted Push-off Mechanism

In this scenario the effects on the separation are observed when the POP of the POM is slightly tilted. Faults during the integration as well as breakdowns during the cruise phase may be reasons for this. To simulate this, a 1-2 mm thick Styrodur wedge is placed between the POP and the bottom plate of the rover. Compliance with the separation corridor must be particularly monitored here.

6.5.8 Scenario 8: Delayed Separation - 50 ms

This scenario will only be necessary under certain conditions. If the scatter of the HDRMs during the nominal separations (Scenario 1) is very small, a artificial created delay of about 50 ms must be added. This can be achieved by varying the pretension of the individual cables.

6.5.9 Scenario 9: Final Shot

In the last scenario, the separation is performed with the flight version of the HDRCs. The rover is equipped with the electronically triggered HDRCs in the more interesting position (0° or 90°). The number of separations depends on the available HDRCs. However, at least one separation of this configuration is performed.

7 Results

The pre-tests described in Chapter 4.1 to determine the release torque showed a maximum required release torque of 5 Nm. Furthermore, these tests showed that the actual required force becomes significantly less once the mechanism is in motion. It is then in the range between 3 and 4 Nm. Unfortunately, the way the reusable HDRC functions does not allow a more precise determination of an exact value. On this basis some calculations were made in Chapter 4 and 6.4.1.

It was calculated that the required release force per HDRM is $F_{req} = 56.12\,\mathrm{Nm}$, if the ratchet wrench's starting angle is at 45°. If a different angle is present, the new projected lever arm can be determined with Equation 4.3. The defined fall height of $s = 0.8\,\mathrm{m}$ also allowed the calculation of the fall time $t = 0.4039\,\mathrm{s}$ and the final velocity $v = 3.9618\,\mathrm{m\,s^{-1}}$. The required mass of the drop weight to ensure a reasonably high safety margin for the release force was also estimated.

Furthermore, an internal document based on the entire Chapter 6 as well as step-by-step instructions on how to prepare and perform the separation tests, is already in preparation.

Due to the postponements already explained in Chapter 5, it has not been possible to include the results of the separation tests in this thesis. The measurement instruments mentioned in Chapter 6.3 will generate a lot of data during testing. By analyzing the data, much will be learned about the rover's separation behavior. The results will include the separation speed and the potential rotation. This will be used to determine the probability of the rover maintaining the required separation corridor. Additionally, the sensitivity of the separation phase is being investigated to see if there is significant change in the rover's rotation or velocity if the trigger delay between the HDRMs grows.
As a result of the separations tests, it is also expected to determine whether off-nominal behavior in the scenarios described in Chapter 6.5 would result in consequences of concern.

8 Discussion

Most of the design requirements, as listed in Chapter 3.2, were met. The MECSS can be easily attached to the modified WCI. In the 0° position as well as in a 90° rotated configuration. For this purpose, the design was constructed very simply and from aluminum profiles, so that a quick adjustment is possible. In this way, it is also possible to react quickly and flexibly to any spontaneous problems that may occur. Furthermore, the external trigger makes it possible to activate the HDRMs simultaneously. The springs play a major part in this, as they compensate for possible differences in the pretensioning of the cables. Possible differences, caused by the uncertain release time along the 90° rotation are kept to a minimum by the rapid release. This is made possible by the drop weight, which first accelerates in free fall and then suddenly pulls on the release cable. This effect is additionally reduced by the pretension using the turnbuckles, as the elastic deformation is already mostly present. One point that has not been clarified yet is the exact approach to delayed release. It still has to be checked, whether it is possible to delay the release of individual HDRMs by varying the pretension in the cable or by adjusting the ratchet wrench's angle.

Almost exclusively standard components were used for the construction. This keeps the costs low and allows flexibility in case something needs to be adapted between separations and scenarios. The spacecraft simulator plate is the only component which is custom made. Every other modification is designed to be quick, easy, inexpensive and - most importantly - can be done in-house. Care was taken to reuse most of the components of the WCI. In addition, it should be considered to keep the profiles longer if possible so that they can be reused in later constructions. This approach also helps with the demand of having potential mounting points for additional cameras or measuring instruments. Due to the vast use of standardized aluminum profiles, the possibilities are almost unlimited to do so.
Even though it has not yet been definitively clarified whether a COR test will take place, the design provides the opportunity to react flexibly to the test demands.

The determined release force is of a magnitude that will work well with the developed design and the chosen spring is the perfect compromise of stiffness and sufficiently visible deflection for the forces that occur. The inaccurate triggering of the HDRMs was initially problematic but should be compensated by the very fast triggering, caused by the accelerated drop weight.
Unfortunately, the adjustment of the WCI could not be realized due to the delay in the test schedule. Preliminary tests to finally verify the functionality of the design must also be carried out later. Because the WCI is already prepared for

the thermal vacuum tests and therefore blocked, the exact mass of the weight must be experimentally determined before the actual separation tests can begin. This ensures that the calculations mentioned here are valid and that damage to the test object can be eliminated.

9 Conclusion

This thesis has shown that separation with the reusable HDRC is still possible. The problem described in Chapter 2 could be solved by the concept presented as far as predictable at the time of submission. Unfortunately, the final implementation as well as the execution of the separation tests did not become part of this thesis. Off-normal behavior, occurring during the early vibrations tests of the SM1, led to an enormous delay of the whole test campaign. Thus, only a fraction of the implementation that actually had to be done made it into this thesis. As a result the associated tests have also slipped to the end of 2022 and could not be further documented here.
Nevertheless, the concept was successfully developed and the required work was prepared as far as possible. The complete test procedure has been elaborated as well as the different scenarios described.

10 Bibliography

[1] Kuramoto, Kiyoshi et al.: "Martian moons exploration MMX: sample return mission to Phobos elucidating formation processes of habitable planets". In: *Earth, Planets and Space* 74.1 (2022), pp. 1–31.

[2] Ulamec, Stephan et al.: "A rover for the JAXA MMX Mission to Phobos". In: *70th InternationalAstronautical Congress*. International Astronautical Federation. 2019, IAC–19.

[3] Vayugundla, Mallikarjuna et al.: "The MMX Rover on Phobos: The Preliminary Design of the DLR Autonomous Navigation Experiment". In: *2021 IEEE Aerospace Conference (50100)*. IEEE. 2021, pp. 1–18.

[4] Grott, Matthias et al.: "In-Situ Radiometric Investigation of Phobos using the MMX Rover's miniRAD Instrument." In: (2022).

[5] Michel, Patrick et al.: "The MMX rover: performing in situ surface investigations on Phobos". In: *Earth, Planets and Space* 74.1 (2022), pp. 1–14.

[6] Bertrand, Jean et al.: "Roving on Phobos: Challenges of the MMX rover for Space Robotics". In: *Proceedings of 15th Symposium on Advanced Space Technologies in Robotics and Automation*. 2019.

[7] Lange, Michael, Grimm, Christian, and Lange, Caroline: "MMX Rover - Drop Test Report". In: (2021).

[8] Glenair: *061-005 Medium-duty hold-down release mechanism*. PDF. Accessed 17-5-2022. 2017. url: https://cdn.glenair.com/space-mechanisms/pdf/a/061-005.pdf.

11 List of Figures

12 List of Tables

13 List of Symbols

Sign	Description	Unit
D	diameter	mm
F	force	N
ID	inner diameter	mm
L_0	length	mm
L	length	mm
OD	outer diameter	mm
S	factor of safety	-
T	torque	N m
Δl	length	mm
α	angle	°
a	acceleration	$\mathrm{m\,s^{-2}}$
c	spring constant	N mm
g	gravitational acceleration	$\mathrm{m\,s^{-2}}$
h	height	mm
m	mass	kg
r	length, lever arm	mm
s	distance	m
t	time	s
t	thickness	mm
v	velocity	$\mathrm{m\,s^{-1}}$
w	width	mm

14 Abbreviations

CAD	Computer Aided Design.
CNES	National Centre for Space Studies.
COR	Coefficient of Restitution.
DAQ	Data Acquisition.
DLR	German Aerospace Center.
FPS	Frames Per Second.
HDRC	Hold Down and Release Component.
HDRM	Hold Down and Release Mechanism.
IMU	Inertial Measurement Unit.
JAXA	Japanese Aerospace Exploration Agency.
LET	Landing and Exploration Technology.
MASCOT	Mobile Asteroid Surface Scout.
MECSS	Mechanical and Electrical Chassis Support System.
MGSE	Mechanical Ground Support Equipment.
miniRad	thermal infrared radiometer.
MLI	Multi Layer Insulation.
MMX	Martian Moons Exploration.
PAC	Pre-Assembled Chassis.
POM	Push-Off Mechanism.
POP	Push-Off Plate.
QM	Qualification Model.
RAX	Raman spectrometer instrument.
SEM	Service Module.
SM	Structure Model.
WCI	Weight Compensation Instrument.

Context of Appendix

GN 585 | Schäkel

geschweifte Ausführung

Ganter Norm®

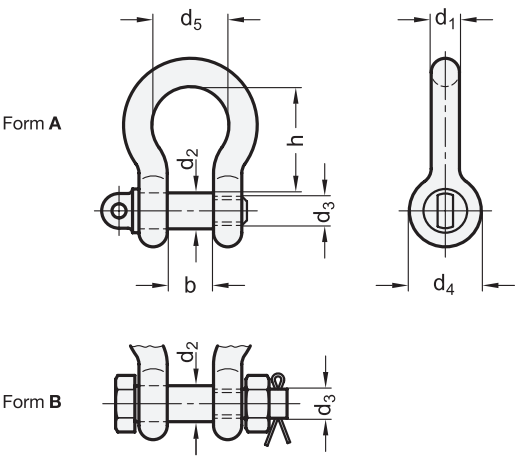

2 Form

A mit Schraubbolzen
B Bolzen mit Mutter und Splint

1

d_1 Nenngröße	in Zoll	b ±1	d_2 ±0,5	d_3 * UNC-Gewinde	d_4	d_5	h	Nenntragfähigkeit (WLL)
6	1/4	12	8	5/16	17	19	28	0,5 t [5,0 kN]
8	5/16	13	10	3/8	21	21	31	0,75 t [7,5 kN]
10	3/8	16	12	7/16	26	24	36	1,0 t [10,0 kN]
11	7/16	18	14	1/2	28	27	42	1,5 t [15,0 kN]
13	1/2	21	16	5/8	30	30	48	2,0 t [20,0 kN]
16	5/8	27	19	3/4	42	38	60	3,25 t [32,5 kN]
19	3/4	32	22	7/8	48	45	71	4,75 t [47,5 kN]
22	7/8	36	25	1	57	51	84	6,5 t [65,0 kN]
25	1	43	28	1 1/8	62	59	95	8,5 t [85,0 kN]

* i. d. R. sind die Bolzen und Schrauben mit dem angegebenen Gewinde versehen. Abweichungen sind jedoch möglich.

Ausführung

- Bügel
  - Vergütungsstahl, gesenkgeschmiedet
  - feuerverzinkt
- Bolzen
  - Vergütungsstahl, gesenkgeschmiedet
  - galvanisch verzinkt, lackiert
- RoHS

Hinweis

Hochfeste, geschweifte Schäkel GN 585 sind in Anlehnung an die US Federal Specification RR-C-271 hergestellt und zeichnen sich durch 6-fache Sicherheit aus. Die Mindestbruchkraft liegt daher mindestens um das 6-fache über dem Wert der Nenntragfähigkeit (WLL). Die geschweifte Form eignet sich besonders für Anwendungen mit Mehrfachbelegung der Schäkel.

Die Nenngröße und die Nenntragfähigkeit (WLL) sind auf dem Schäkel eingeschmiedet, was die sichere Zuordnung des Anschlagmittels erleichtert. Generell darf die Nenntragfähigkeit nicht überschritten werden.

Die Ausführung mit Mutter und Splint (Form B) wird in der Regel für andauernde Verbindungen empfohlen. Die Bolzen können sich drehen und die Muttern sind gegen unbeabsichtigtes Lösen durch einen Splint gesichert.

Weitere Anwendungsrichtlinien enthält die Betriebsanleitung, die jedem Schäkel beigefügt ist (siehe auch unter www.ganternorm.com/de/service).

Bestellbeispiel		
GN 585-11-B	1	d_1
	2	Form

061-005

Medium-duty hold-down release mechanism

2500 lb. release preload
Electrically redundant

ELECTRICALLY REDUNDANT HOLD DOWN RELEASE MECHANISM, MEDIUM DUTY

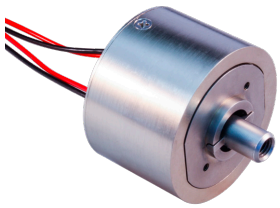

How To Order		
Sample Part No.	**061**	**-005**
Basic Part No.	Light/Medium Duty HDRM	
Dash No.	Redundant Circuit	

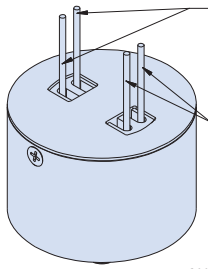

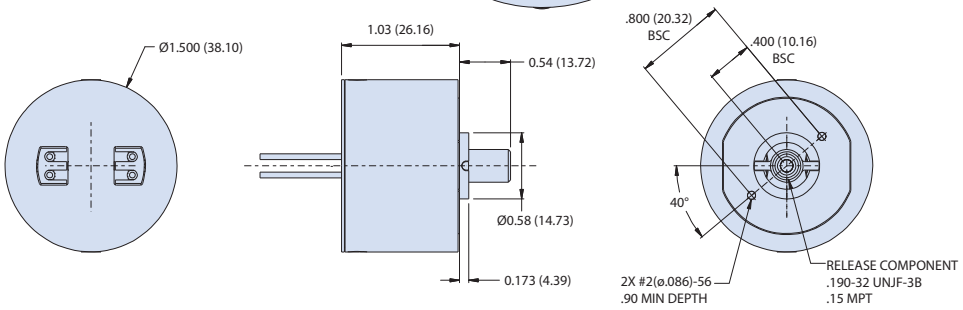

Physical characteristics	
Mass	84.9 grams nominal weight
Release component thread	0.190-32 UNJF-3B*
Material list	IAW MSFC-STD-3029
Epoxy	Outgassing requirements per GSC19384
Device features	
Redundant initiation	2 initiation points
Field refurbishable	Initiator can be replaced in less than 15 minutes by trained personnel
Reliability prediction	0.9999994
Packaging	External housing typically supplied with two mounting points. Custom housings and mountings available
Connectorization	Standard design supplied with wire inputs. Connectorized versions available
Scalable bolt size	Bolt size determines preload and can be scaled to accommodate a wide range of requirements
*Size callout based on the bolt size to be used. Metric thread also available. Consult factory for qualification test report.	

NOTES

1. Unit is identified with Glenair name, CAGE code, part number, and date code, space permitting. Primary initiation circuit identified with "P" and redundant with "R".
2. Release preload 2500 lbs. (11.1 kN)
3. Reference Glenair P/N 060-105 for refurbishment initiator
4. Nominal actuation current 3.5 Amps
5. Metric threads available, consult factory for options

061-005

Medium-duty hold-down release mechanism

2500 lb. release preload
Summary of qualification test data

A

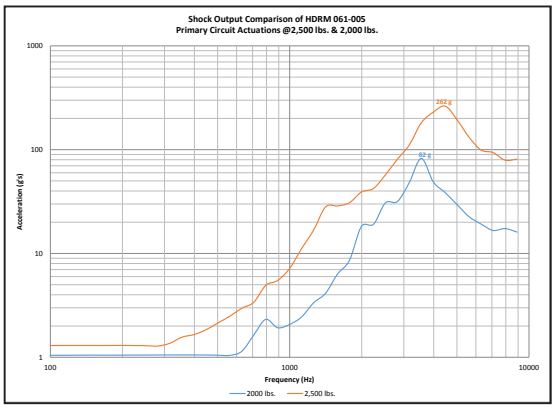

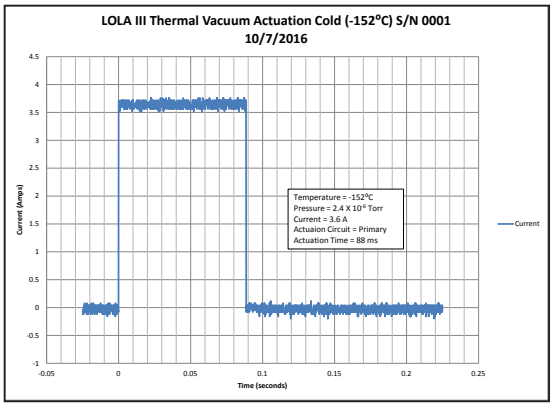

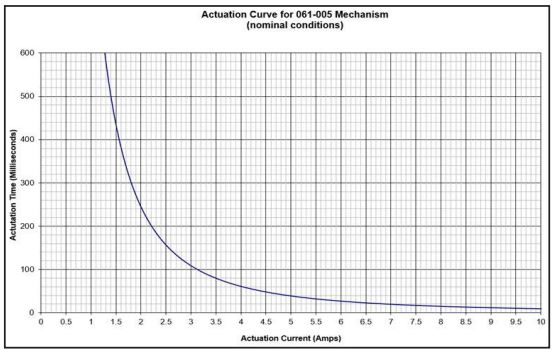

Tested Capability for 061-005	
Nominal Release Preload	2,250 pounds
Proof Preload	2,500 pounds
Ultimate Load	3,250 pounds
Electrical Resistance	1.5 ohms max
Sine Vibration 3 orthogonal axes	25 G's
Random Vibration 3 orthogonal axes	50.9 G_{rms}
Actuation Time	Under 100 ms @3.5 Amps
Shock Input	2,849 G's
Source Shock	Under 300 G's @2,500 pounds
Life Test	10 refurbishments during qualification and an expected continued usage
Temperature	-150°C to +150°C released in a vacuum (1x10-6 Torr)
Extended Preload	<4.0% loss

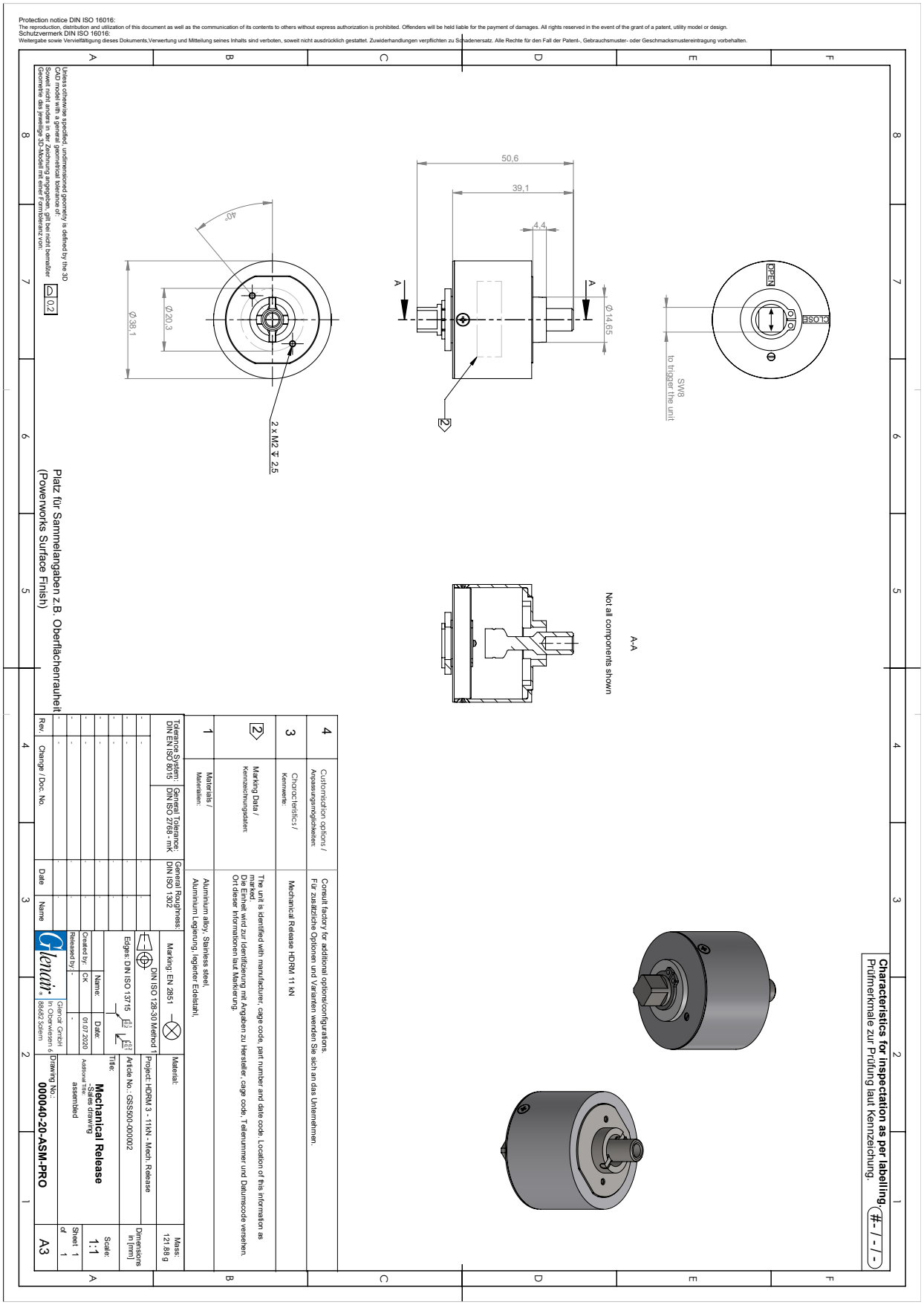
Protection notice DIN ISO 16016:
The reproduction, distribution and utilization of this document as well as the communication of its contents to others without express authorization is prohibited. Offenders will be held liable for the payment of damages. All rights reserved in the event of the grant of a patent, utility model or design.
Schutzvermerk DIN ISO 16016:
Weitergabe sowie Vervielfältigung dieses Dokuments,Verwertung und Mitteilung seines Inhalts sind verboten, soweit nicht ausdrücklich gestattet. Zuwiderhandlungen verpflichten zu Schadenersatz. Alle Rechte für den Fall der Patent-, Gebrauchsmuster- oder Geschmacksmustereintragung vorbehalten.
Unless otherwise specified: undimensioned geometry is defined by the 3D CAD model
Soweit nicht anders in der Zeichnung angegeben, gilt hier nicht bemaßter Geometrie das jeweilige 3D-Modell mit einer Formtoleranz von:
0.2
Platz für Sammelangaben z.B. Oberflächenrauheit (Powerworks Surface Finish)
50,6
39,1
4,4
Ø14,65
Ø38,1
Ø20,3
40°
2 x M2 ↧ 2,5
SW8
to trigger the unit
OPEN
CLOSE
A-A
Not all components shown
Characteristics for inspectation as per labelling
Prüfmerkmale zur Prüfung laut Kennzeichnung.
#- / -
4 Customisation options / Anpassungsmöglichkeiten: Consult factory for additional options/configurations. Für zusätzliche Optionen und Varianten wenden Sie sich an das Unternehmen.
3 Characteristics / Kennwerte: Mechanical Release HDRM 11 kN
2 Marking Data / Kennzeichnungsdaten: The unit is identified with manufacturer, cage code, part number and date code. Location of this information as marked. Die Einheit wird zur Identifizierung mit Angaben zu Hersteller, cage code, Teilenummer und Datumscode versehen. Ort dieser Informationen laut Markierung.
1 Materials / Materialien: Aluminium alloy, Stainless steel). Aluminium Legierung, legierter Edelstahl).
Tolerance System: DIN EN ISO 8015
General Tolerance: DIN ISO 2768 -mK
General Roughness: DIN ISO 1302
Marking: EN 2851 DIN ISO 128-30 Method 1
Edges: DIN ISO 13715
Rev. | Change / Doc. No. | Date | Name
Created by: C.K 01.07.2020
Released by: -
Glenair GmbH In Oberwiesen 6 88682 Salem
Material:
Project: HDRM 3 - 11kN - Mech. Release
Article No.: GSS500-000002
Title: Mechanical Release
Additional Title: -Safed drawing assembled
Drawing No.: 000040-20-ASM-PRO
Mass: 121.88 g
Dimensions in (mm)
Scale: 1:1
Sheet 1 of 1
A3

Edelstahl Drahtseil

DIN 13414-1 | V4A AISI 316

Drahtseil Durchmesser	Konstruktion	Gewicht/Meter	Mindestbruchkraft	Zugfestigkeit
		kg	kN	N/mm²
0,5mm	7x7	0,002	0,15	1570
1mm	7x7	0,004	0,61	1570
1mm	1x19	0,004	0,82	1570
1,5mm	7x7	0,009	1,37	1570
1,5mm	1x19	0,009	1,85	1570
2mm	7x7	0,013	2,44	1570
2mm	1x19	0,013	3,30	1570
3mm	7x19	0,031	5,10	1570
3mm	1x19	0,031	7,42	1570
4mm	7x19	0,055	8,34	1570
4mm	1x19	0,055	13,20	1570
5mm	7x19	0,086	13,00	1570
5mm	1x19	0,086	20,60	1570
6mm	7x19	0,130	18,80	1570
6mm	1x19	0,130	29,70	1570
8mm	7x19	0,243	33,30	1570
10mm	7x19	0,359	56,80	1570

Edelstahl Drahtseilklemme

DIN EN 741 | V4A AISI 316

EDELSTAHL® Rost frei

Bügelform, poliert

Maße gemäß Zeichnung (mm)

Seildurchmesser	Gewicht/Stk	Gewinde	Höhe	Abstand Mitte Bolzen	Anziehdrehmoment	Mindestanzahl Seilklemmen
	kg	d_1	h_1	a	Nm	pro Endverbindung
2mm	0,007	M3	19mm	7,70mm	2,00	3
3mm	0,012	M3	20mm	8,50mm	2,00	3
4mm	0,013	M4	22mm	10,40mm	2,00	3
5mm	0,014	M5	25mm	11,80mm	2,00	3
6mm	0,017	M6	34mm	13,70mm	3,50	4
8mm	0,041	M6	37mm	16,40mm	6,00	4
10mm	0,080	M8	46mm	19,20mm	9,00	4

Der Abstand „e" zwischen den Drahtseilklemmen soll min. 1,5x und nicht mehr als 3x der Breite der Klemmbacke betragen.

Bei Verwendung einer Kausche in der Schlaufenkonstruktion sollte die erste Drahtseilklemme unmittelbar an der Kausche angebracht werden.
Die Klemmbacke sollte immer auf dem belasteten Teil des Seil angebracht werden.

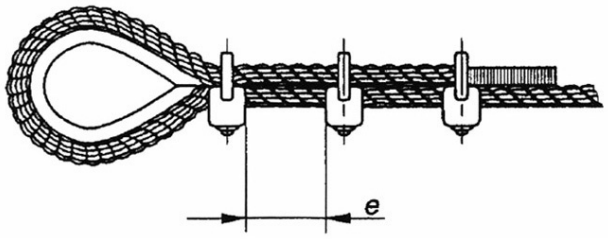

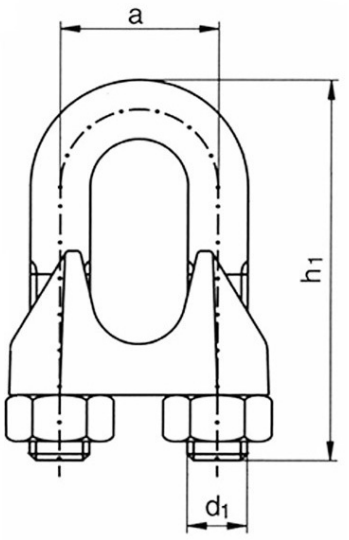

Edelstahl Karabinerhaken

DIN 5299 | Form C

Hochglanzpoliert
mit Schnapphaken

Maße gemäß Zeichnung (mm)

Nenngröße	Nutzlast	Gewicht/Stk	Durchmesser	Materialstärke	Innere Breite	Öffnung	Länge
		kg	d_2	d_1	f	m	l
40 x 4	50kg	0,011	6mm	4mm	4mm	7mm	40mm
50 x 5	120kg	0,016	8mm	5mm	4mm	7mm	50mm
60 x 6	120kg	0,029	9mm	6mm	6mm	8mm	60mm
70 x 7	180kg	0,044	10mm	7mm	8mm	8mm	70mm
80 x 8	230kg	0,069	12mm	8mm	8mm	10mm	80mm
10 x 100	350kg	0,129	15mm	10mm	10mm	11mm	100mm
11 x 120	450kg	1,129	18mm	11mm	11mm	16mm	120mm

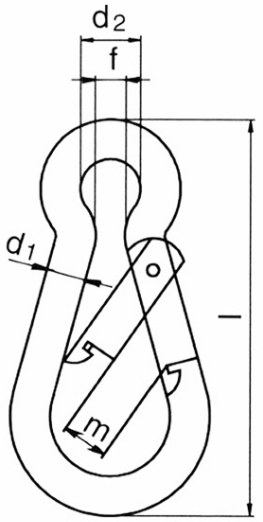

Edelstahl Klemmstopper

V4A AISI 316

1-teilig mit Madenschraube

Maße gemäß Zeichnung (mm)

Seildurchmesser	Gewicht/Stk	Durchmesser	Höhe	Gewinde
	kg	D	A	M
2mm	0,013	10mm	8mm	M4
3mm	0,013	15mm	12mm	M8
4mm	0,014	15mm	12mm	M8
5mm	0,030	20mm	15mm	M10
6mm	0,030	20mm	15mm	M10

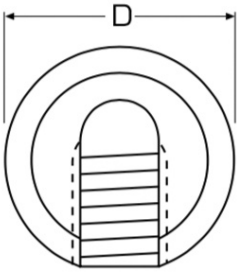

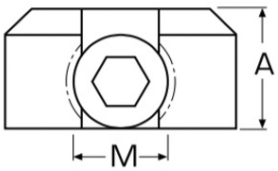

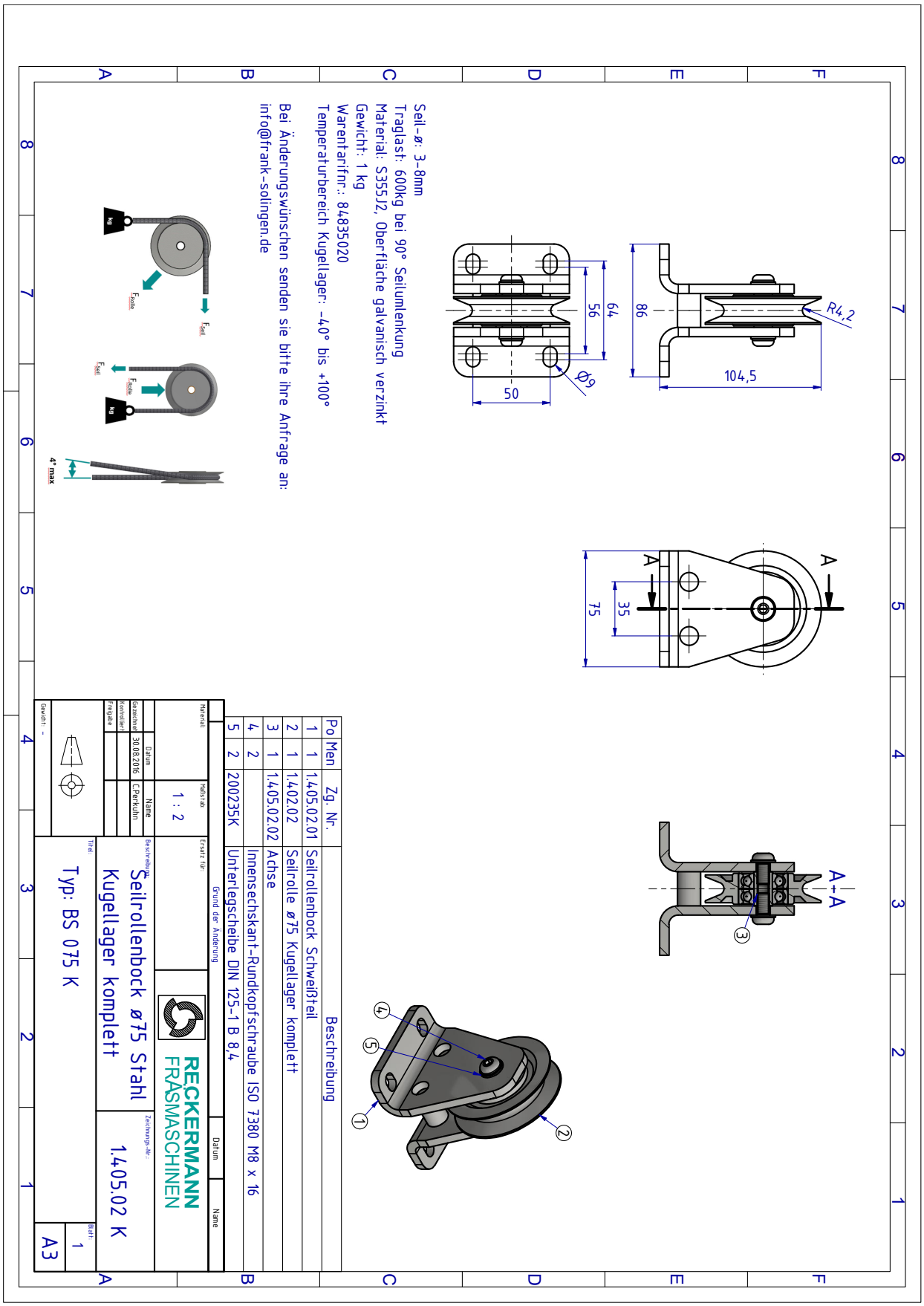
Seil-ø: 3-8mm
Traglast: 600kg bei 90° Seilumlenkung
Material: S355J2, Oberfläche galvanisch verzinkt
Gewicht: 1 kg
Warentarifnr.: 84835020
Temperaturbereich Kugellager: -40° bis +100°
Bei Änderungswünschen senden sie bitte ihre Anfrage an:
info@frank-solingen.de
R4,2
86
104,5
64
56
50
Ø9
A
A
75
35
A-A
4° max
Po Men Zg. Nr. Benennung
1 1 1.405.02.01 Seilrollenbock Schweißteil
2 1 1.402.02 Seilrolle ø75 Kugellager komplett
3 1 1.405.02.02 Achse
4 2 Innensechskant-Rundkopfschraube ISO 7380 M8 x 16
5 2 200235K Unterlegscheibe DIN 125-1 B 8,4
Material
Maßstab 1 : 2
Ersatz für:
Grund der Änderung
Datum
Name
Datum
Name
30.08.2016
C.Perkuhn
Gezeichnet
Kontrolliert
Freigabe
Gewicht: -
Titel
Typ: BS 075 K
Benennung
Seilrollenbock ø75 Stahl
Kugellager komplett
Zeichnungs-Nr.:
1.405.02 K
Blatt
1
A3

DryLin® R Linear - Product range

Round flange, pillow block - iglide® J liner

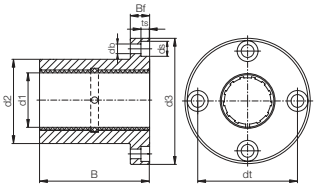

Order key

Type						Size
F	J	U	M	-	01	- 10
Flange	iglide® Material	Liner	Metric	Round		Diameter

Dimensions [mm]

Part No.	d1	d2 h7	d3	dt	B	Bf	ts	db	ds
FJZM-☐-08	8	16	32	24	25	8	3.1	3.5	6.0
FJUM-☐-10	10	19	39	29	29	9	4.1	4.5	7.5
FJUM-☐-12	12	22	42	32	32	9	4.1	4.5	7.5
FJUM-☐-16	16	26	46	36	36	9	4.1	4.5	7.5
FJUM-☐-20	20	32	54	43	45	11	5.1	5.5	9.0
FJUM-☐-25	25	40	62	51	58	11	5.1	5.5	9.0
FJUM-☐-30	30	47	76	62	68	14	6.1	6.6	11.0
FJUM-☐-40	40	62	98	80	80	18	8.1	9.0	14.0
FJUM-☐-50	50	75	112	94	100	18	8.1	9.0	14.0

Technical Data

Part No.	d1-Tolerance[78] [mm]	F max. dynamic[82] P = 5 MPa [N]	F max. static[82] P = 35 MPa [N]	Weight [g]
FJZM-☐-08	+0.032 +0.070	960	6,720	20
FJUM-☐-10	+0.030 +0.088	725	5,075	32
FJUM-☐-12	+0.030 +0.088	960	6,720	42
FJUM-☐-16	+0.030 +0.088	1,440	10,080	51
FJUM-☐-20	+0.030 +0.091	2,250	15,750	88
FJUM-☐-25	+0.030 +0.091	3,625	25,375	152
FJUM-☐-30	+0.040 +0.110	5,100	35,700	266
FJUM-☐-40	+0.040 +0.115	8,000	56,000	552
FJUM-☐-50	+0.050 +0.130	12,500	87,500	853

Supplement the part number with one of the following choices.
Example: FJUM-01-10 LL for a standard version

For Standard version use 01
For Low Clearance version use 31

Also available with liners:


TUM-01


JUM-11


E7UM-01

[78] According to igus® testing method ➤ Page 1096
[82] Design standards ➤ Page 1001
Please note: Installation instructions ➤ Page 1003

3D-CAD files, prices and delivery time ➤ www.igus.com/drylinR

1083

Schraubenzugfedern - Artikelnummer Febrotec: 0E0750-0952500S

[E0750-095-2500S | 2,41x19,05x63,5xA2 | 80887S | X750095250 | OE0750-0952500S]

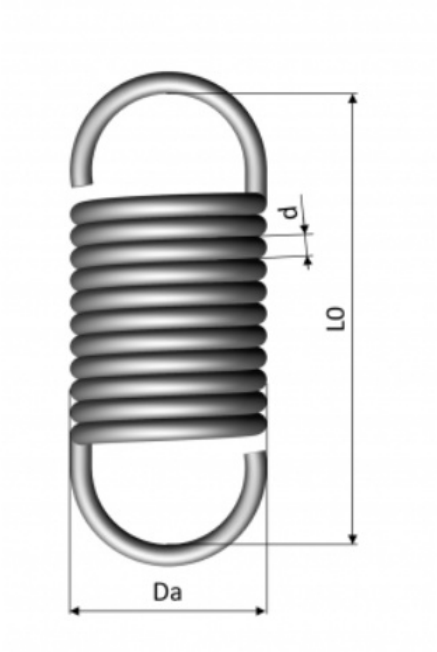

Aussen ø	Da	19.05 [mm]
Draht ø	d	2.41 [mm]
Länge	L0	63.5 [mm]
Vorspannung	Fo	13.75 [N]
Prüflänge	L1	91.95 [mm]
Kraft bei L1	F1	152.74 [N]
Federrate	c	4.860 [N/mm]
Werkstoff		1.4310
Gewicht		29.274 [g]